LBL-12812
Preprint

Lawrence Berkeley Laboratory
UNIVERSITY OF CALIFORNIA

Materials & Molecular Research Division

OCT 9 1981

Submitted to the Journal of Catalysis

METHANE PRODUCTION FROM THE CATALYZED REACTION OF GRAPHITE AND WATER VAPOR AT LOW TEMPERATURES (500-600 K)

A.L. Cabrera, Heinz Heinemann, and G.A. Somorjai

August 1981

TWO-WEEK LOAN COPY

This is a Library Circulating Copy which may be borrowed for two weeks. For a personal retention copy, call Tech. Info. Division, Ext. 6782.

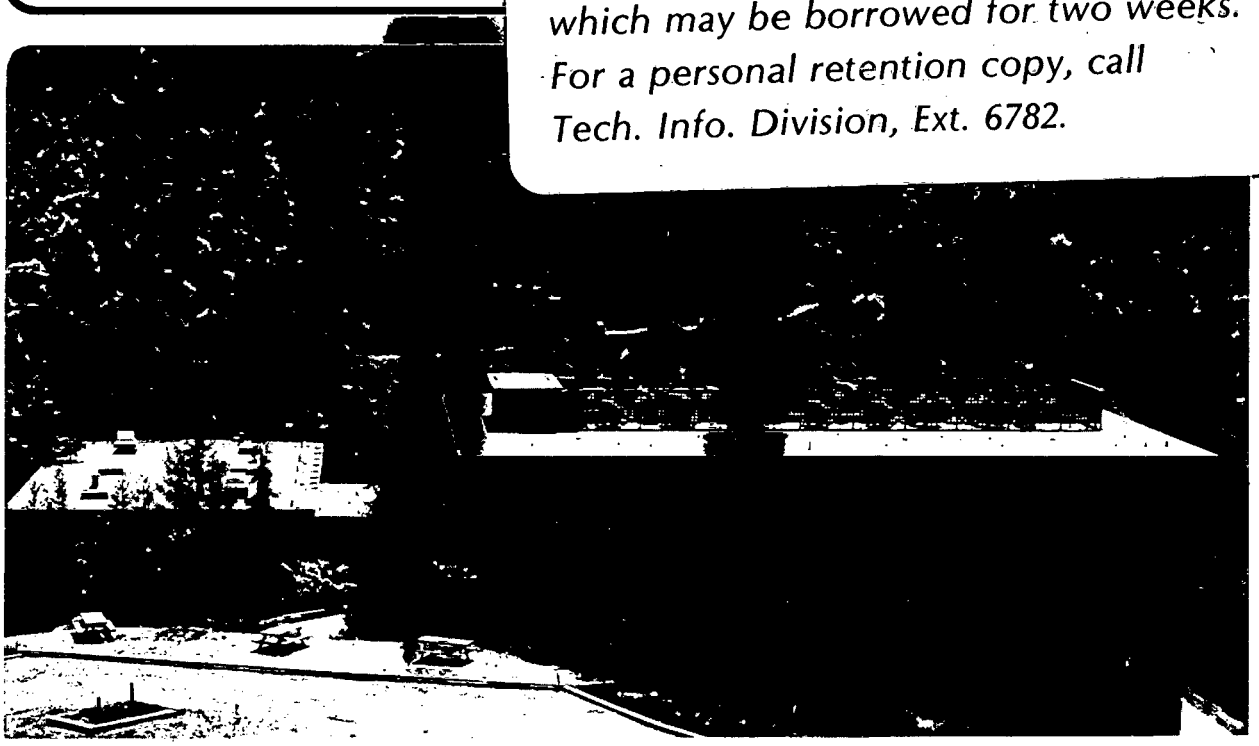

Prepared for the U.S. Department of Energy under Contract W-7405-ENG-48

LBL-12812 c.2

DISCLAIMER

This document was prepared as an account of work sponsored by the United States Government. While this document is believed to contain correct information, neither the United States Government nor any agency thereof, nor the Regents of the University of California, nor any of their employees, makes any warranty, express or implied, or assumes any legal responsibility for the accuracy, completeness, or usefulness of any information, apparatus, product, or process disclosed, or represents that its use would not infringe privately owned rights. Reference herein to any specific commercial product, process, or service by its trade name, trademark, manufacturer, or otherwise, does not necessarily constitute or imply its endorsement, recommendation, or favoring by the United States Government or any agency thereof, or the Regents of the University of California. The views and opinions of authors expressed herein do not necessarily state or reflect those of the United States Government or any agency thereof or the Regents of the University of California.

LBL 12812

METHANE PRODUCTION FROM THE CATALYZED REACTION OF GRAPHITE AND WATER VAPOR AT LOW TEMPERATURES (500-600 K)

A.L. Cabrera, Heinz Heinemann, and G.A. Somorjai

Materials and Molecular Research Division, Lawrence Berkeley Laboratory, and Department of Chemistry, University of California, Berkeley, CA 94720

Abstract

The steady state production of methane from the catalyzed reaction of high density graphite and water vapor at low temperatures (500-600 K) is reported. The reaction is catalyzed by potassium hydroxide and potassium carbonate placed on the graphite surface. The steady state production of methane has a turnover frequency of $10^{-3}sec^{-1}$ at 522 K and an activation energy of 10 ± 3 kcal/mole. Several other alkali hydroxides, lithium, sodium, and cesium hydroxide all turned out to be good catalysts for the production of methane from water vapor and graphite. The surface composition and surface texture were characterized by Auger electron spectroscopy and scanning electron microscopy, respectively.

This work was jointly supported by the Director, Office of Basic Energy Research, Office of Basic Energy Sciences, Chemical Sciences Division, and the Assistant Secretary for Fossil Energy, Office of Coal Research, Liquefaction Division of the U.S. Department of Energy under Contract No. W-7405-ENG-48 through the Pittsburgh Energy Technology Center, Pittsburgh, PA.

Introduction

The production of low molecular weight gaseous hydrocarbons directly from carbon or from various carbonaceous deposits (coal, unburned particulates, biomass) provides an intriguing alternative to liquefaction with hydrogen or to gasification to carbon monoxide and hydrogen at high temperatures (>1000 K). The reaction of carbon with water to produce methane and carbon dioxide,

$$2C + 2H_2O \rightarrow CH_4 + CO_2 \qquad (1)$$

is virtually thermoneutral ΔG_{600K}=+3(kcal/mole) and thermodynamically feasible at low temperatures. Nevertheless, much of the research carried out to convert carbon to hydrocarbon liquids has concentrated on high presssure reactions with hydrogen. Studies of coal gasification with water proved that high temperature regimes were needed for efficient production of CO and H_2 [1]. While recent studies by Mims and Pabst [2] reported the production of substantial amounts of CH_4 along with CO and H_2 during coal gasification using K_2CO_3 as a catalyst, these studies have still employed relatively high temperatures (>900 K) which facilitate the decomposition of most hydrocarbons that would be produced.

Our research is focused on finding suitable catalysts for low temperature production of low molecular weight hydrocarbon molecules from carbon (coal). We report the efficient conversion of high density graphite to methane and CO_2 using potassium compounds as catalysts in the temperature range of 500 to 600 K. The reaction has a turnover frequency of 10^{-3} sec^{-1} at 522 K. While most of our studies have been carried out using clean graphite samples of ~ $1cm^2$, scale-up to produce large concentrations of methane appears feasible by using graphite powder with a much larger area. The potassium catalyzed methane production was studied over samples of high density graphite. The samples were either covered with potassium that was

evaporated from an external source, in situ, in ultrahigh vacuum (UHV) or by impregnation with KOH or K_2CO_3, obtained from their respective solutions, prior to introducing the samples into the UHV chamber. In all three cases the steady state rates of production of CH_4 were the same. Potassium also catalyzes the water-gas shift reaction:

$$CO + H_2O \rightarrow CO_2 + H_2 \qquad (2)$$

in the temperature range 300-600 K; the K_2CO_3 covered graphite catalyzed this reaction (2) better than KOH-covered graphite.

Several other alkali hydroxides were also utilized as catalysts to compare their activity for the methane production with that of potassium hydroxide. Lithium hydroxide (LiOH) yielded the highest rate of CH_4 production; the cesium hydroxide (CsOH) activity was comparable to that of potassium hydroxide and sodium hydroxide (NaOH) was the least active catalyst.

Experimental

Several samples of graphite were cleaved in air with a razor blade from a larger piece of highly oriented pyrolytic graphite (HOPG) obtained from Union Carbide Corporation. The high density material contained no hydrogen or oxygen. The samples were cut to a rectangular shape having geometric areas ranging from 0.65 to 1.00 cm^2 and a thickness of ~ 1 mm. The graphite sample was then mounted on the manipulator of a UHV system operating at a base pressure $<10^{-9}$ torr. The graphite is held from both ends by gold wires.

When the sample holder was positioned properly inside the system, the sample surface was accessible to surface composition analysis by Auger electron spectroscopy (AES), ion sputter cleaning, and mass spectrometry. AES was performed with a cylindrical mirror analyzer from Physical Electronics Industries, Inc. that was mounted on moveable bellows. The system was also

equipped with a high pressure cell which isolates the sample and allows us to perform chemical reaction studies at high pressures (up to 100 atm) without removing the sample from the UHV chamber. The product distribution obtained at high pressures were monitored by an HP 5880A gas chromatograph with a thermal conductivity detector and a six foot column of Chromosorb 102 in series with a six foot column of Chromosorb 101. This chromatographic column combination resolves H_2, CO, CH_4 and CO_2 at room temperature and H_2O when the gas chromatograph oven is heated to 150°C after the CO_2 peak has evolved. The graphite samples were heated resistively by a high current AC power supply and the sample temperature monitored with a chromel-alumel thermocouple inserted between the graphite and one of the gold leads. This system is an improved version of a high pressure-low pressure instrument reported earlier [3]. A schematic diagram of the system with the high pressure cell closed or open is shown in Figure 1.

Half a monolayer of potassium was deposited onto the graphite using a potassium-zeolite gun at a background pressure of 1×10^{-9} torr. This potassium source consisted of a platinum filament coated with a potassium-aluminosilicate emitter and a collimator, similar to that described by Marbrow and Lambert [4]. The potassium coverage of the sample was determined by monitoring the growth of the potassium layer on a piece of gold foil as a function of time by means of AES. Plotting the potassium Auger peak intensity at 252 eV as a function of deposition time, a layer-by-layer growth mechanism [5] was obtained. Once the time of deposition to form a half monolayer was determined, potassium was evaporated onto the graphite using identical experimental conditions. After the half monolayer of potassium was deposited onto the graphite, the high pressure cell was closed and the sample was exposed to a mixture of water vapor and helium. This mixture consisted of 30 torr

of vapor obtained from distilled water and 1 atm of high purity helium that was further purified by using a liquid nitrogen trap. The potassium covered graphite was then heated to the desired temperature in this gas mixture and the gas composition was analyzed every 10 minutes with the gas chromatograph for 4 to 24 hours. The cleanliness of the graphite surface and the potassium surface concentration was monitored by AES before and after the high-pressure experiments.

In another case, a solution of KOH with a molarity of 0.38 M was prepared, and the fresh sample of graphite already mounted on the manipulator was dipped into the solution and then dried in air. The KOH covered graphite sample was then exposed to high vacuum for AES analysis. Once the cleanliness of the surface was checked, the isolation cell was closed and the sample was exposed to the water-helium gas mixture and heated to the desired temperature. The products' concentrations were measured with the gas chromatograph and the reaction was carried out under the same conditions used with the potassium covered graphite samples. The sample surface was analyzed by AES before and after the experiments. This procedure was repeated at different reaction temperatures, each time using a fresh sample of graphite. When samples of graphite were coated with other alkali hydroxides (LiOH, NaOH, CsOH) or with K_2CO_3, solutions of these bases were made with the same molarity (0.38 M) as in the case of KOH, and the same procedure was used.

Thermal desorption experiments were performed using an EAI mass spectrometer for the detection of the different desorption products. The mass spectrometer ionizer was placed at 5 cm from one of the sample faces; a nearly constant heating rate of 10 K/sec was employed in the range 300-1200 K to desorb the adsorbates.

A quartz microreactor technique [6] was employed to measure methane

production from graphite powder impregnated with KOH. The purpose of these studies was to prove that the catalyzed production of CH_4 from graphite and water vapor could be readily scaled up to produce large quantities of CH_4.

In our apparatus, a mixture of helium and water was flowed over the sample which was placed in a temperature controlled reactor. The exit of the reactor was attached to the sampling valve of the gas chromatograph and the gas flow vented to the atmosphere. Water vapor saturated helium was obtained by bubbling a stream of helium through a closed container filled with distilled water. The partial pressure of water was ~ 40 torr and the total pressure inside the reactor was ~ 1 atm. The reactor consisted of a 6 mm o.d.x4 mm i.d.x30 cm long quartz tube in a tube furnace, the temperature of which could be regulated to within ± 5 K. The powdered graphite with KOH was held in the reactor tube with glass wool plugs. A chromel-alumel thermocouple enclosed in a thin walled 3 mm o.d. quartz tube was inserted in one side of the reactor tube, making direct contact with the sample to monitor its temperature. This system is described in more detail elsewhere [7].

Results and Discussion

K-graphite system. (Half a monolayer of potassium deposited on graphite).

No chemical reaction between graphite and water vapor is detectable in the absence of the potassium catalyst. In the presence of potassium the production of CH_4 can be readily observed when this system is heated to 473 K. The concentrations of CH_4, CO_2, and CO produced during the reaction of water vapor with the graphite samples were monitored as a function of time in the temperature range of 475-600 K. Hydrogen was detected among the reaction products, but due to the similarity of its thermal conductivity to that of the carrier gas (He), it was difficult to quantitatively

follow its concentration change. The buildup of CH_4 concentration at two temperatures, 475 and 523 K, is displayed in Figure 2. There is an initial high rate of methane production that, after about an hour, settles to a somewhat slower steady state rate that can be maintained for extended periods of time in the temperature range 473-523 K. From this figure and similar data obtained at other temperatures, an activation energy for the production of CH_4 of 10 ± 3 Kcal/mole can be estimated. The turnover frequency for the methane formation reaction is about 10^{-3} sec^{-1} at 523 K, assuming that all the graphite surface atoms are active.

The concentration of CO_2 and CO that accumulated in the reaction chamber were about 10 and 30 times higher, respectively, than the CH_4 concentration. In order to determine whether there were other sources than graphite for the formation of the detected reaction products in the high pressure chamber, several blank experiments were performed. A gold foil with and without potassium was substituted for the high density graphite sample in the chamber and the experiments were repeated using identical conditions of water vapor pressures and temperature. No methane could be detected in this case. However, production of CO_2 and CO could be observed at rates which are not too different from those detected in the presence of graphite. It appears that the walls of the stainless steel reaction chamber provide a source of carbon for carbon oxide formation in the presence of water vapor. In order to obtain carbon mass balance for the graphite-water reaction that produces methane, the amounts of CO_2 and CO produced by the blank experiments must be subtracted from the total amount of CO_2 and CO detected under reaction conditions. The relative buildup of CO and CO_2 concentrations obtained with either the gold foil or with the graphite samples for the two temperatures, (475 and 523 K), is displayed in Figures 3 and 4, respectively. In

the case of CO production, the concentration appears to be independent of temperature, and after subtracting the amount produced in the blank experiment there is no CO left within experimental error. However, the CO_2 concentration does depend on temperature and, after subtraction of the amount produced in the blank experiments, some CO_2 still remained, as seen in Figure 4. This amount of CO_2 is equivalent to the CH_4 concentration produced at the same temperature. Therefore, the reaction that produces CH_4 and CO_2 may be expressed as: $2H_2O + 2C\ (\text{graphite}) \xrightarrow{K} CH_4 + CO_2$ (at 473-673 K).

The graphite-water reaction was studied in the temperature range of 473-673 K, and it was found that the highest conversion to CH_4 occurs at 523 K. Up to this temperature the rate of CH_4 production occurs in a steady state and there is no sign of catalyst poisoning. At temperatures above 523 K the potassium Auger peak diminishes with time and the surface is covered with an increasing concentration of carbonaceous species as detected by AES; simultaneously, the production of CH_4 slows down and then stops. After completion of a run, potassium was not readily detectable by AES. The graphite was then flashed at 1200 K and a strong peak of CO was obtained in the mass spectrometer with a maximum desorption rate at ~ 900 K, as shown in Figure 5. In the same figure we show a CO desorption spectrum (dashed curve) from a sample of pure graphite, with the same geometric area, which was exposed to ~ 100 L of CO. Carbon monoxide is only weakly adsorbed on pure graphite and in much smaller concentration. Once the CO is termally desorbed from the sample or removed by argon ion bombardment, potassium is detected once more (with AES) and on reaction with water the CH_4 production starts up again. When using a mixture of 1 atm of CO with 30 torr of water vapor on the K-covered graphite, only H_2 and CO_2 formation could be detected,

indicating that the water-gas shift reaction was taking place and that the methanation reaction was inhibited. In the presence of a gas mixture of 1 atm of CO_2 and 30 torr of water vapor, no products of any kind were detected.

The KOH-graphite system.

The production of CH_4 was studied using graphite samples that were dipped in 0.38 M KOH solution and then air-dried. The water vapor pressure in the H_2O/He mixture was the same as used previously, and our experiments were carried out in the temperature range 475-568 K. The accumulation of CH_4 as a function of time at various temperatures are displayed in Figure 6. These curves exhibit larger initial rates of CH_4 production than those measured for the Kgraphite system which appears in the first five minutes after the sample is heated to the preset temperature. Nevertheless, in steady state (after the initial burst) the methane production rates are identical. A plot of the logarithm of the steady state rates obtained from Fig. 6 divided by the number of carbon atoms of the graphite sample as a function of the inverse absolute temperature is shown in Fig. 7. From this plot an activation energy for the CH_4 production of 11.9 ± 0.5 kcal/mole is obtained. This activation energy is in good agreement with the 10 ± 3 kcal/mole that was estimated for the CH_4 production using the K-graphite system.

The CO and CO_2 concentrations were also monitored in this case. Most of the CO present in the gas phase is again CO desorbed from the high pressure cell walls and in the presence of water it readily reacts to form H_2 and CO_2 by means of the water-gas shift reaction (Eq.2). The water-gas shift reaction achieves its maximum rate in the CO_2 and H_2 production

at ~ 525 K and then at higher temperatures slows down and stops completely at ~ 568 K. The CO and CO_2 concentrations measured are displayed in Figs. 8 and 9, respectively. In Fig. 9 we have also plotted the CO_2 produced by the water-gas shift reaction which occurs at room temperature, 298 K, (detectable CH_4 production starts up only at 475 K). No CO_2 is produced at 568 K. On the other hand, the CO concentration (Fig. 8) which remained almost independent of temperature and similar to that detected on a gold foil, covered with potassium, clearly is increased at 568 K, when CO_2 is no longer produced, indicating that the water-gas shift reaction is inhibited. This suggests that at these high temperatures the KOH catalyzed water vapor-graphite reaction produces primarily gaseous CH_4 and CO.

$$2H_2O + 3C\ (\text{graphite}) \xrightarrow[568\ K]{KOH} CH_4 + 2CO \qquad (3)$$

Even though Eq. 3 is not thermoneutral at low temperatures, it becomes thermodynamically more favorable at high temperatures (ΔG_{400K}=26 kcal/mole; ΔG_{600K}=14 kcal/mole).

In order to show more clearly the selectivities of the various reactions of water vapor over the KOH-graphite system, we have plotted the rate of CH_4, CO_2, and CO produced under our reaction conditions as a function of temperature in Fig. 10. In this figure the CO_2 production rate corresponds to the rate of the water-gas shift reaction. The CO_2 produced along with the CH_4 according to Eq.1 was very difficult to estimate because the CO_2 produced in the water-gas shift reaction (almost 90% of the total CO_2) was very sensitive to the KOH concentration on the surface of the graphite or on the gold foil used in blank experiments. Surface composition analysis by AES indicated a reduction in the intensity of the potassium peak (252 eV) after

the sample was exposed to reaction conditions.

In order to learn about the structure of the active graphite surface and about the state of dispersion of KOH, samples of graphite coated with KOH were inspected by a scanning electron microscope (SEM) before and after being exposed to reaction conditions. Initially, the KOH crystallites cover the surface of the graphite fairly uniformly forming a weblike network as seen in Fig. 11a. After it is exposed to the reaction conditions, KOH agglomerates forming crystallites of a few microns in diameter, scattered over the graphite surface, as indicated in Fig. 11b. Thus the KOH-graphite contact area is markedly reduced. One can also notice in Fig. 11b roughened patches that were absent before the water-graphite reaction. These patches are perhaps the locations where graphite was chemically attacked and produced CH_4.

The reduction in the contact surface between KOH and graphite is likely to be responsible at least in part for the reduced CH_4 rate of production after an initial period and for the steady state rate being appreciably lower than the initial reaction rate.

In order to ascertain that the CH_4 production from KOH-graphite was catalytic, the production of CH_4 at 522 K was measured for a period of 20 hours and is plotted in Fig. 12. The rate of CH_4 evolution stays constant at turnovers greater than 10 molecules per site. In order to scale up methane production by using higher surface area samples, graphite powder impregnated with KOH was placed in a quartz reactor and a mixture of water and helium was introduced at a flow rate of 30 cc/min. The temperature of the oven was raised to 522 K and after a period of 1 min. methane was readily detected.

The behavior of methane production in this flow reactor was the same as

previously observed with the high pressure-low pressure system; a burst of methane was detected during the first 10 minutes of reaction time, then the CH_4 production rate slowed down and reached a steady state. Whenever the graphite powder was impregnated with fresh KOH, a new burst of CH_4 was detected. This behavior can either be explained by the reduction of the contact surface between the graphite and the KOH, or by KOH undergoing a chemical transformation into a potassium compound which is less active in catalyzing this reaction.

The K_2CO_3-graphite system

This sytem was studied in detail at only two temperatures, 495 K and 522 K, since it behaves similarly to the potassium-graphite systems previously investigated. The CH_4 production at these two temperatures is plotted as a function of time in Fig. 13. In this same figure we have plotted the steady state production of CH_4 from the KOH-graphite system at the same temperatures.

The KOH-graphite and K_2CO_3-graphite behave identically in the steady state production of CH_4 as indicated in this figure. The CO_2 and CO concentrations are plotted in Figs. 14 and 15, respectively. Much more CO_2 is produced because the water-gas shift reaction is better catalyzed by K_2CO_3-graphite than by the KOH-graphite system at the same temperature (see Fig. 14). We have also plotted in this figure the CO_2 produced at 495 K in a blank experiment (when graphite is replaced by a gold foil coated with K_2CO_3) as represented by open hexagons. It seems that at low temperatures, the mechanism responsible for the CH_4 production can be described once more by the reaction represented by Eq. 1. The CO buildup in the gas phase is now higher than in the previous cases; nevertheless, the blank experiment per-

formed with gold foil at 495 K yields the same CO concentration, indicating that no CO was produced from the graphite-water reaction in the temperature range 400-600 K. In order to clarify this point, thermal desorption experiments were performed from K_2CO_3-coated gold foil, suspecting that the extra CO buildup in the cell could come from the decomposition of the potassium carbonate. It was found that CO desorbed from K_2CO_3 at two temperatures, 356 K and 482 K, and that the real decomposition of the carbonate did not start until ~ 900 K, in good agreement with results obtained by other researchers [8]. Once the K_2CO_3 was degassed, no CO peaks at low temperatures were obtained. Therefore, the extra CO found in the cell was CO chemisorbed on the K_2CO_3, when the K_2CO_3-graphite samples were prepared outside the reaction cell. The strong chemisorption of CO by this system also explains its high activity towards the water-gas shift reaction. Potassium surface concentration measured by AES before and after reaction show a reduction in the potassium Auger peak intensity (252 eV) after the sample was exposed to reaction conditions, but this decrease in the potassium intensity is less significant than in the case of the KOH-graphite system.

The LiOH-, NaOH-, and CsOH-graphite systems.

Different samples of graphite coated by impregnation with 0.38 M solutions of LiOH, NaOH, and CsOH were studied as potential methanation catalysts and compared with the KOH-graphite system. These samples were studied at 522 K and all of the alkali hydroxides proved to be good catalysts for the production of methane from water and graphite. The experimental conditions were identical to those used for the K, KOH, K_2CO_3-graphite systems. The CH_4 concentration at 522 K is plotted as a function of time in Fig. 16. One can see that KOH-, CsOH-, and NaOH-graphite yielded nearly the same CH_4

production rates in the steady state, but LiOH-graphite is clearly more active. On the other hand, the initial rate of CH_4 production follows the sequence CsOH, KOH, NaOH, and LiOH from the highest to the lowest initial rate. Once the rate of methanation is calculated per carbon site, the turnover frequency obtained for LiOH-graphite is almost 2.5 times higher than CsOH-graphite and KOH-graphite, and about 4 times higher than NaOH-graphite (Table I). It should be noted that the activity of these hydroxides for CH_4 production at low temperatures follows the same correlation as the activity of the corresponding carbonates for graphite gasification at high temperatures as studied by McKee and Chatterji [9]. These samples were also inspected by scanning electron microscopy, and crystallite formations containing the alkali metals were found in all cases after the samples were exposed to reaction conditions. The average size of the crystallites follows the same sequence as the initial rate of CH_4 production; the largest crystallites were found in the case of CsOH ~ 30 μ m; sizes for KOH were ~ 10 μ m; for NaOH and LiOH ~ 4 μ m.

The CO_2 and CO concentrations obtained in these experiments are displayed in Figs. 17 and 18, respectively. In the LiOH-graphite and NaOH-graphite systems no CO_2 was produced, indicating that CH_4 formation occurs according to Eq.3. No attempt was made in this case to measure the CO or CO_2 buildup in a blank experiment.

Thermal Desorption Experiments

Thermal desorption experiments were performed over a piece of gold foil coated with KOH in order to study the thermal stability of this hydroxide. The base pressure of the system was $<10^{-9}$ torr before the gold was resistively heated up to 1200 K at a rate of 10 K/sec. The hydrogen, oxygen, and

potassium peaks were scanned with the mass spectrometer during heating. The evolution of H_2 was detected around 400 K and potassium (mass 39) was detected at a higher temperature, 775 K, as shown in Fig 19, but no O_2 (mass 32) was detected until the temperature of ~ 990 K was reached. The desorption of metallic potassium from graphite takes place at about the same temperature as from gold. Since KOH is very stable toward dissociation [10], hydrogen evolution at 400 K might come from the dissociation of chemisorbed water over this system. The potassium peak is detected near the temperature range at which KOH vaporized. The high flux of K^+ ions is a result of KOH cracking due to ionization [10].

H_2 desorption

One of the intermediate steps in the production of CH_4 is the formation of CH_x complexes on the surface of the graphite. If one interrupts the production of CH_4 from the alkali hydroxide-graphite systems, the surface of the samples should have adsorbed CH_x complexes which, upon heating, will decompose to yield molecular hydrogen (desorbing to the gas phase) and leaves carbon atoms on the surface. This decomposition must take place at high temperatures because of the formation of strong bonds by carbon and hydrogen atoms. Salmeron and Somorjai [11] studied the decomposition of unsaturated hydrocarbons on the Pt(111) crystal face and they found that the complete dehydrogenation of these hydrocarbon fragments took place between 550-710 K. Therefore, each of the systems studied in the CH_4 production was flashed to 1200 K, after the reaction with water. A strong hydrogen peak was detected at high temperatures. Thermal desorption spectra of hydrogen desorption from LiOH-, NaOH-, KOH-, and CsOH-graphite are displayed in Fig. 20.

In order to make sure that the H_2 was not hydrogen from the alkali

hydroxide compounds, a piece of gold foil was coated with the different alkali hydroxides and flashed in ultrahigh vacuum up to 1200 K. H_2 was detected at much lower temperatures in each case and these desorption spectra are also displayed in Fig. 21. From these figures one can see that hydrogen desorption from CsOH and KOH takes place below the reaction temperature studied (522 K); hydrogen desorption from LiOH takes place above that temperature and, finally, NaOH has two weak desorption peaks, one above and one below 522 K.

Conclusions

The production of gaseous CH_4 and CO_2 (or CH_4 and CO) from graphite occurs rapidly in the temperature range 500-650 K with a low activation energy (10 ± 3 kcal) in the presence of alkali compounds. KOH, K_2CO_3, LiOH, CsOH, and NaOH all appear to catalyze both the reduction of C to CH_4 and its oxidation to CO_2 or CO. This is a process of considerable complexity that requires many sequential reaction steps. The dissociation of water to OH^- and H^+ is clearly catalyzed by alkali hydroxides, as indicated by studies of the photodecomposition of H_2O vapor on $SrTiO_3$ surfaces [12]. This reaction proceeds at 300 K only in the presence of alkali hydroxides which catalyze the hydroxylation of the oxide surface. Thus the alkali hydroxides aid what must be one of the first reaction steps, the dissociation of H_2O on the graphite surface. The OH^- and H^+ produced in this way then participate in the multiple step oxidizing and reducing reactions. H^+ appears to form C-H bonds and sequential addition of H atoms, and the breaking of C-C bonds are needed to form the CH_4 molecule. The OH^- is able to donate its oxygen to produce C-O bonds and eventually desorbed CO_2 or CO. The use of high density oxygen-free graphite rules out the possibility that hydrogen or oxygen in

the final gaseous products, CH_4 and CO_2, can come from sources other than the water molecules.

Further studies aimed at exploring the mechanism of this catalyzed reaction include attempts to detect CH_x and COH intermediates by electron spectroscopy and exploration of the possibility of K intercalation into the graphite that may be an important reaction step needed to break the C-C bonds of the reactant efficiently. The use of alkaline earth compounds as possible catalysts will be investigated to optimize the activity of the carbon-water ($C-H_2O$) reaction. The combination of transition metals and alkali-metal compounds as catalysts should be explored in order to aid the formation of gaseous hydrocarbon molecules other than CH_4.

Using high surface area graphite, we have shown that scaling up the $C-H_2O$ reaction to produce large amounts of CH_4 gas can readily be accomplished. Thus this reaction can be carried out under technologically feasible conditions. One should then consider other, more economical sources of carbon to produce CH_4, such as coal, biomass, including wood or other plant sources. In these systems, part of the hydrogen that is to be converted to CH_4 would be supplied in part by the hydrocarbons in the carbon source.

Another interesting carbon source is the particulates emitted from internal combustion engines. It appears possible to aid the catalyzed gasification of this carbonaceous material using alkali hydroxide or other suitable catalysts.

Since alkali compounds and water vapor are abundant and readily available on the surface of our planet, one could perhaps associate the presence and accumulation of CH_4 in certain areas such as in coal mines with the $C-H_2O$ reaction that occurs at relatively low temperatures and with low activation energy.

Acknowledgement

This work was jointly supported by the Director, Office of Energy Research, Office of Basic Energy Sciences, Chemical Sciences Division, and the Assistant Secretary for Fossil Energy, under Contract Number W-7405-ENG-48, through the Pittsburgh Energy Technology Center, Pittsburgh, PA

References

1. Wen-Yang Wen, Catal. Rev. Sci. Eng. 22, 1 (1980).

2. C.A. Mims and J.K. Pabst, Amer. Chem. Soc. Abstract papers presented, Div. of Fuel Chemistry, Vol. 25, No.3, p. 258 (1980).

3. D.W. Blakely, E.I. Kozak. B.A. Sexton, and G.A. Somorjai, J. Vac. Sci. & Technol. 13, 1091 (1976).

4. R.A. Marbrow and R.M. Lambert, Surface Sci. 6, 329 (1976).

5. G.E. Rhead, J. Vac. Sci. & Technol. 13, No. 2, 603 (1976).

6. R.J. Kokes, H. Tobin and P.H. Emmett, J. Amer. Chem. Soc. 77, 5860 (1955).

7. C.A. Luengo, A.L. Cabrera, H. B. MacKay, and M. B. Maple, J. Catal. 47, 1 (1977).

8. B.J. Wood, K.M. Sancier, K.H. Lau, D.R. Sheridan, and H. Wise, The Mechanism of Catalytic Gasification of Coal Char, Technical Progress Report No. 2, March, 1981, SRI Project 2202.

9. D.W. McKee and D. Chatterji, Carbon 13, 381 (1975).

10. R.J. Porter and R.C. Schoonmaker, J. Phys. Chem. 62, 234 (1958).

11. M. Salmeron and G.A. Somorjai, to be published.

12. F.T. Wagner and G.A. Somorjai, Nature 285, 559 (1980).

Table 1. Methane reaction rates of the water-graphite reaction catalyzed by various alkali hydroxides

System	Geometric surface area of graphite sample (cm^2)	Rate of CH_4* production (molecule/carbon Surface atom x sec).
LiOH-grahite	0.77	23.8×10^{-4}
NaOH-graphite	0.81	5.6×10^{-4}
KOH-graphite	0.72	9.9×10^{-4}
CsOH-graphite	0.65	10.0×10^{-4}

* It was assumed 1×10^{15} sites per 1 cm^2 of graphite.

Figure captions

Figure 1. (a) Schematic diagram of the apparatus with high pressure cell closed, (b) detail with high pressure cell open.

Figure. 2 Number of CH_4 molecules produced during the potassium catalyzed water-graphite reaction as a function of time for two different temperatures.

Figure 3. Number of CO molecules produced as a function of time for two different temperatures. Open circles and triangles correspond to blank experiments performed with potassium-covered gold foils. Full circles and triangles correspond to experiments with potassium-covered graphite in the reaction chamber.

Figure 4. Number of CO_2 molecules produced as a function of reaction time for two different temperatures. Dashed curved corespond to blank experiments performed with potassium-covered gold foil. Solid lines correspond to experiments with potassium-covered graphite in the reaction chamber.

Figure 5. Thermal desorption of CO from the K-graphite system after it was exposed to reaction conditions. Dashed curve corresponds to CO desorption from pure graphite after it was exposed to 100 L of CO.

Figure 6. Number of CH_4 molecules produced during the KOH catalyzed water-graphite reaction as a function of reaction time for various temperatures.

Figure 7. Logarithm of the CH_4 production rate as a function of the inverse absolute temperature for the KOH-graphite system.

Figure 8. Number of CO molecules produced during the KOH catalyzed water-graphite reaction as a function of reaction time for various temperature.

Figure 9. Number of CO_2 molecules produced during the KOH catalyzed water-graphite reaction as a function of reaction time for various temperatures. Open circles correspond to the production of CO_2 from the KOH catalyzed water-gas shift reaction which takes place at room temperature.

Figure 10. Plot of the rates of CH_4, CO_2, and CO production during the KOH catalyzed water-graphite reaction as a function of absolute temperature.

Figure 11. SEM micrographs of KOH on graphite (a) before exposure to reaction conditions, (b) after exposure to reaction conditions.

Figure 12. Number of CH_4 molecules produced during the KOH catalyzed water-graphite reaction as a function of reaction time, measured at 522 K for 20 hours.

Figure 13. Number of CH_4 molecules produced during the K_2CO_3 and KOH catalyzed water-graphite reactions as a function of reaction time for two different temperatures. For the KOH catalyzed reaction, only the steady state production of CH_4 is plotted.

Figure 14. Number of CO_2 molecules produced during the K_2CO_3 and KOH catalyzed water-graphite reactions as a function of reaction time for two different temperatures. Open hexagons correspond to a blank experiment performed with K_2CO_3-covered gold foil at 495 K.

Figure 15. Number of CO molecules produced during the K_2CO_3 and KOH catalyzed water-graphite reactions as a function of reaction time for two different temperatures. Open hexagons, open triangles, and open circles correspond to blank experiments performed with K_2CO_3- and KOH-covered gold foils at various temperatures. Open squares correspond to pure graphite at 495 K.

Figure 16. Number of CH_4 molecules produced during the LiOH,NaOH, KOH, and CsOH catalyzed water-graphite reactions as a function of reaction time at 522 K.

Figure. 17 Number of CO_2 molecules produced during the K_2CO_3, KOH, and CsOH catalyzed water-graphite reactions as a function of time at 522 K.

Figure 18. Number of CO molecules produced during the LiOH, NaOH, KOH, and CsOH catalyzed water-graphite reactions as a function of reaction time at 522 K. Open squares correspond to pure graphite at the same temperature.

Figure 19. Thermal desorption of H_2 and K from a KOH-covered gold foil sample.

Figure 20. Thermal desorption of H_2 from LiOH-, NaOH-, KOH-, and CsOH-graphite samples after exposure to reaction conditions.

Figure 21. Thermal desorption of H_2 from LiOH-, NaOH-, KOH-, and CsOH-covered gold foil samples.

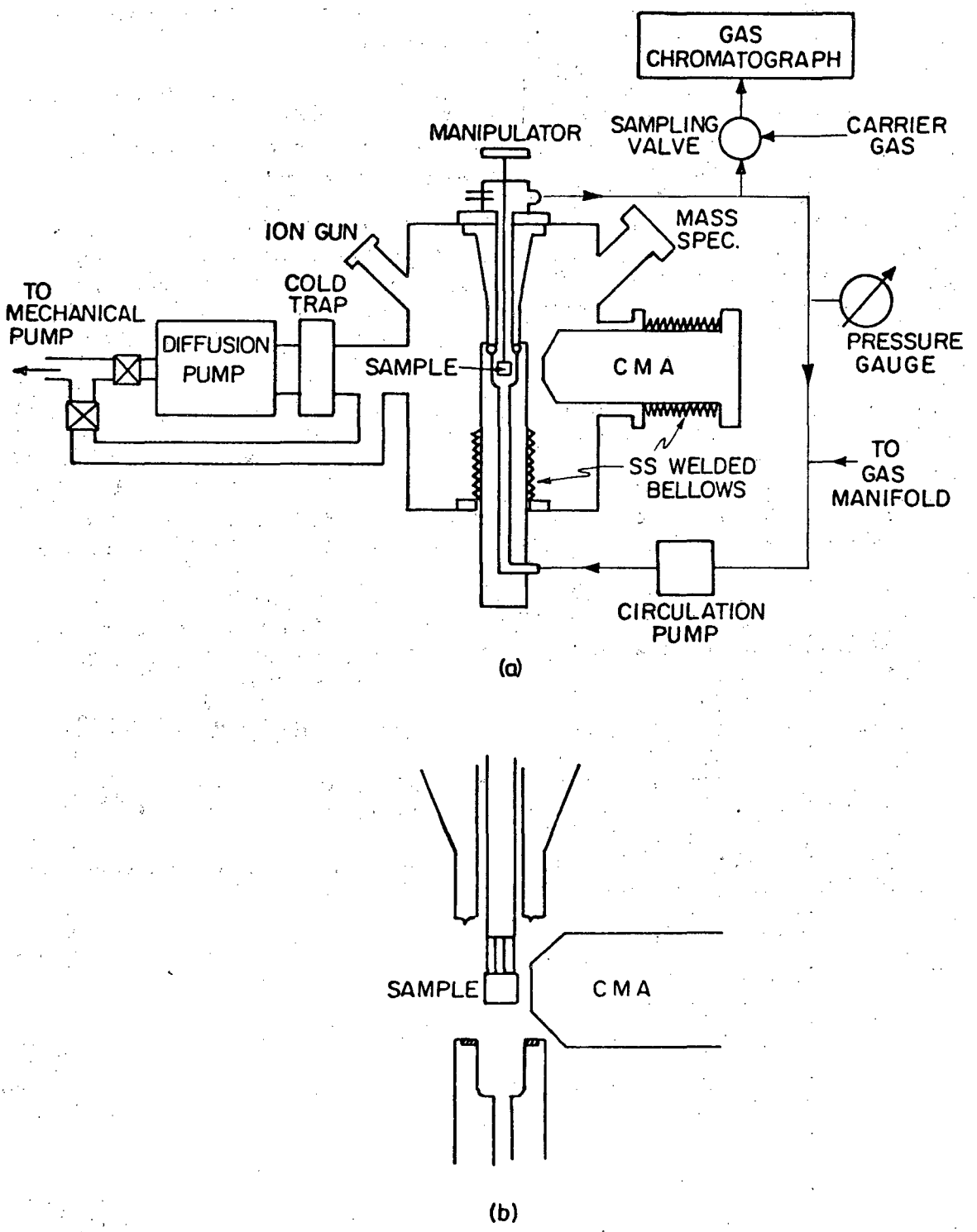
GAS
CHROMATOGRAPH
MANIPULATOR
SAMPLING
VALVE
CARRIER
GAS
ION GUN
MASS
SPEC.
TO
MECHANICAL
PUMP
COLD
TRAP
DIFFUSION
PUMP
SAMPLE
C M A
PRESSURE
GAUGE
SS WELDED
BELLOWS
TO
GAS
MANIFOLD
CIRCULATION
PUMP
(a)
SAMPLE
C M A
(b)
XBL 814-5584

Fig. 1

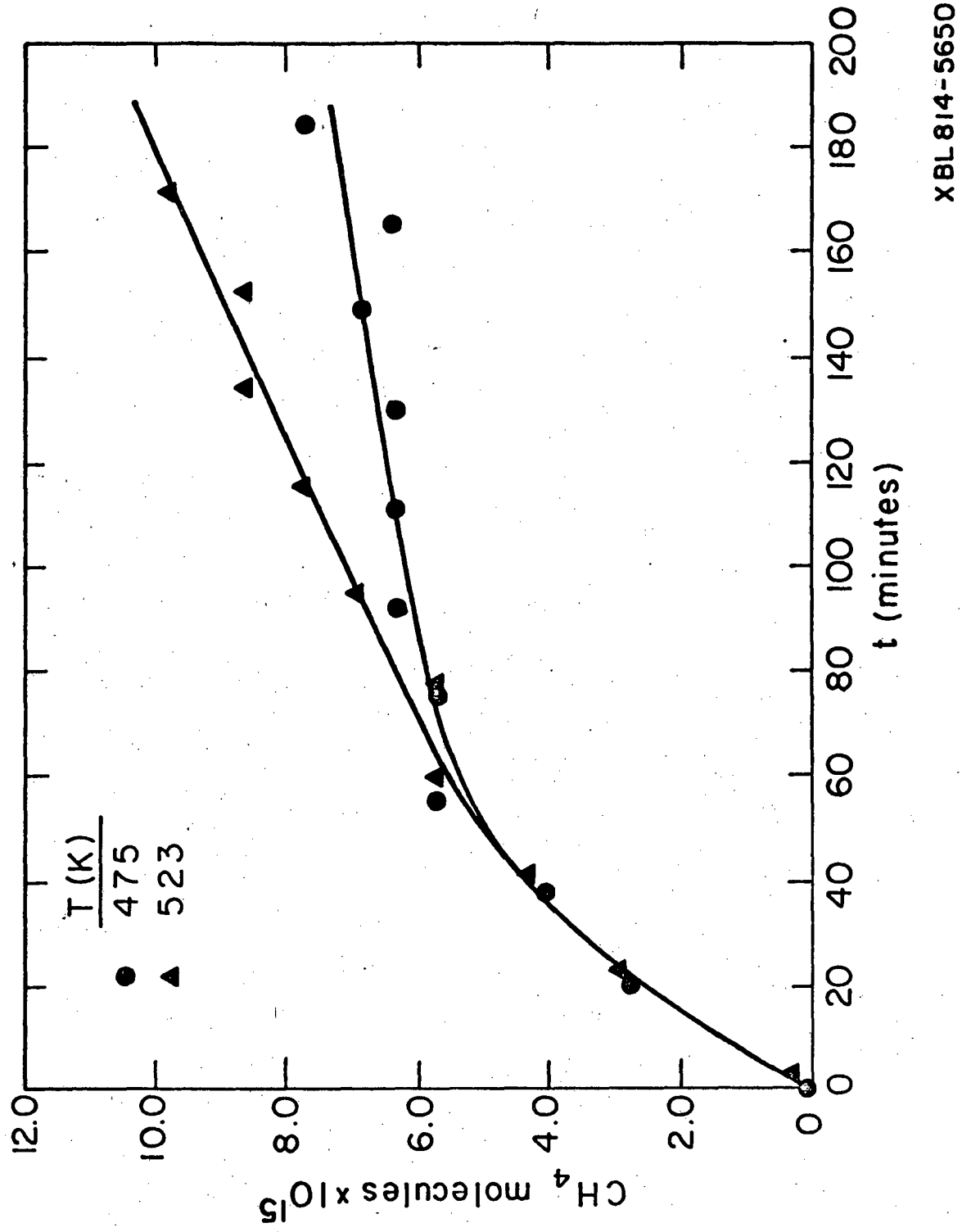
T (K)
475
523
CH4 molecules x 10^15
12.0
10.0
8.0
6.0
4.0
2.0
0
0
20
40
60
80
100
120
140
160
180
200
t (minutes)
XBL 814-5650

Fig.2

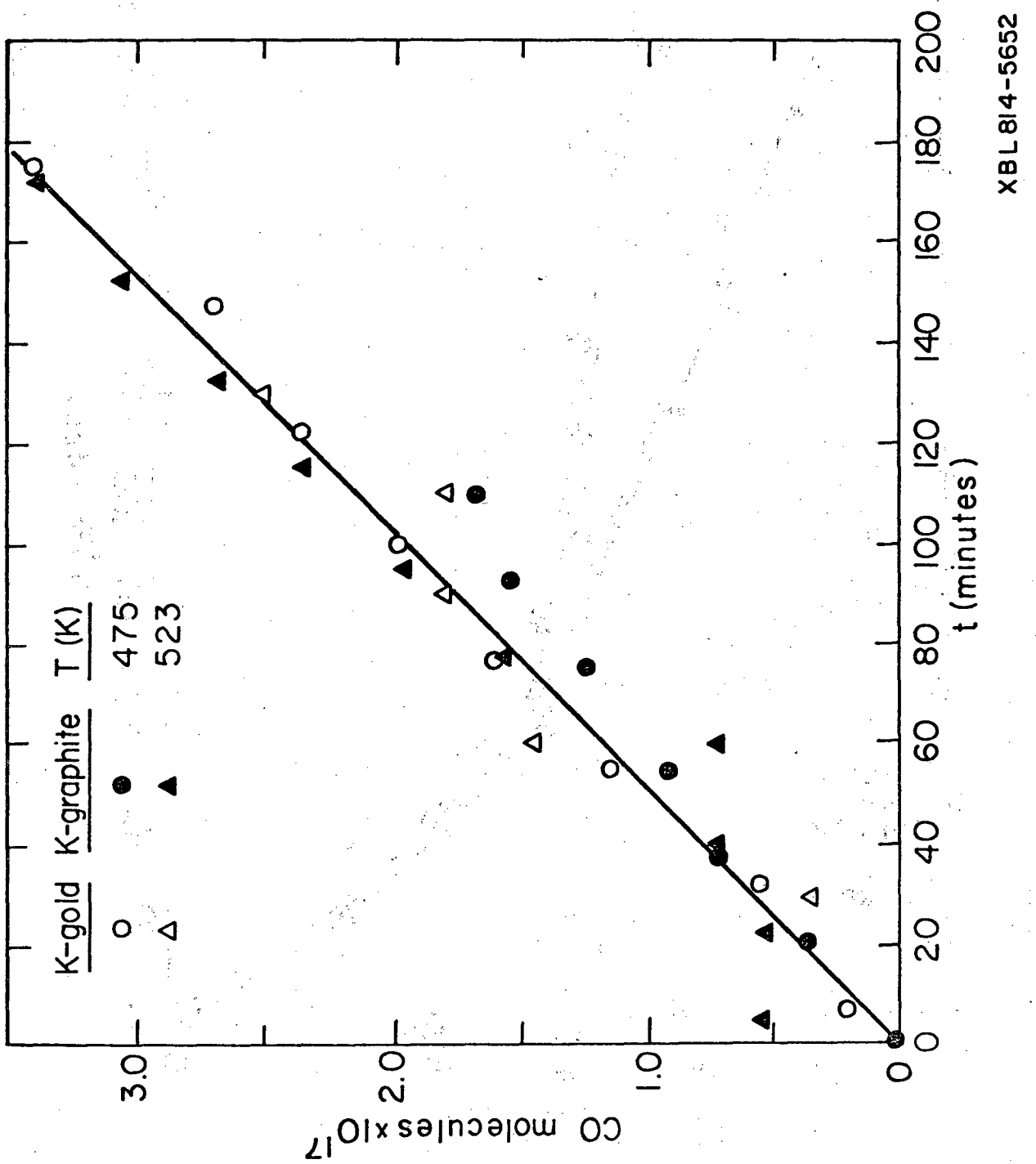
K-gold
K-graphite
T (K)
475
523
CO molecules x10^17
3.0
2.0
1.0
0
0
20
40
60
80
100
120
140
160
180
200
t (minutes)
XBL 814-5652

Fig.3

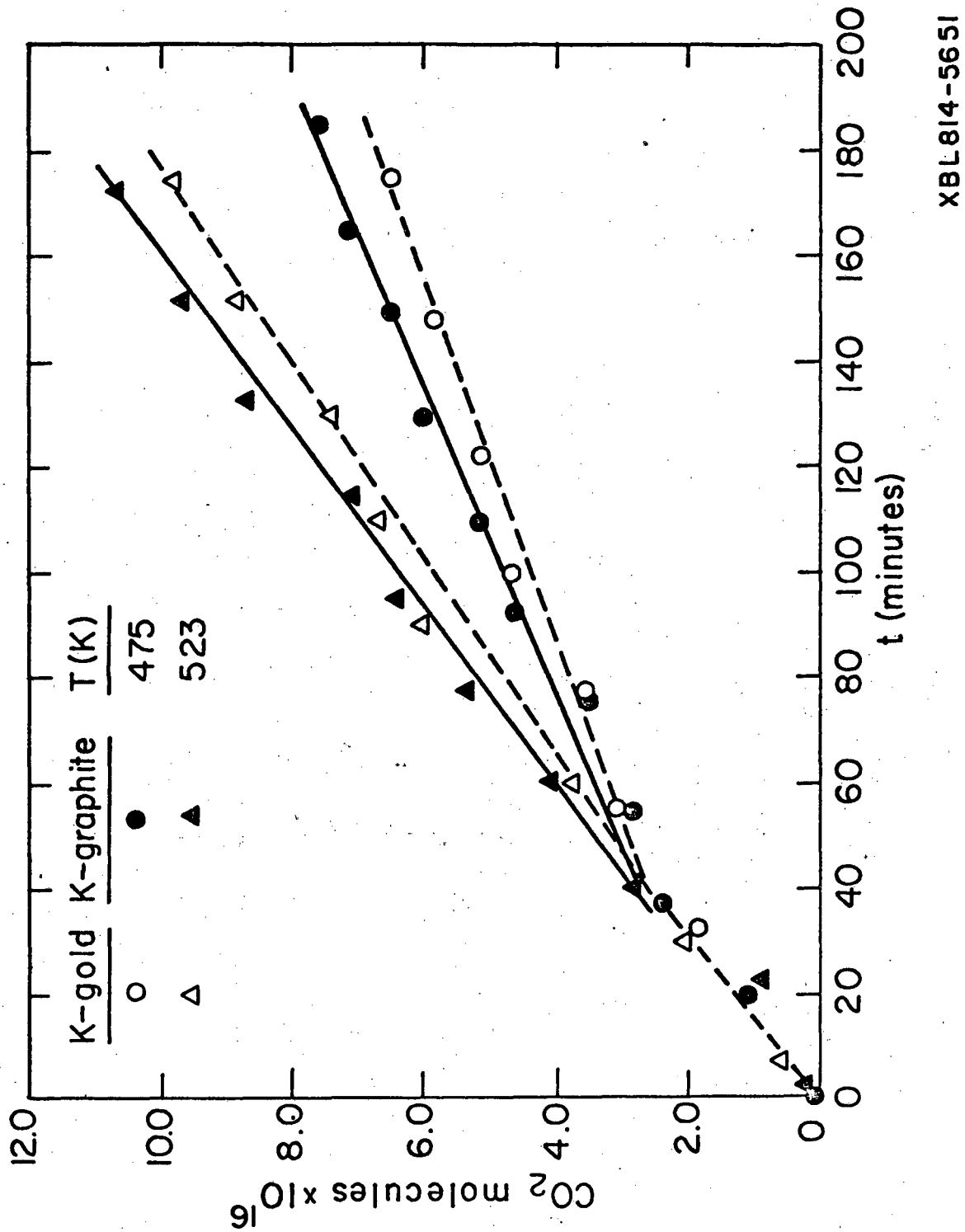
K-gold
K-graphite
T (K)
475
523
CO_2 molecules x 10^{16}
12.0
10.0
8.0
6.0
4.0
2.0
0
0
20
40
60
80
100
120
140
160
180
200
t (minutes)
XBL814-5651

Fig.4

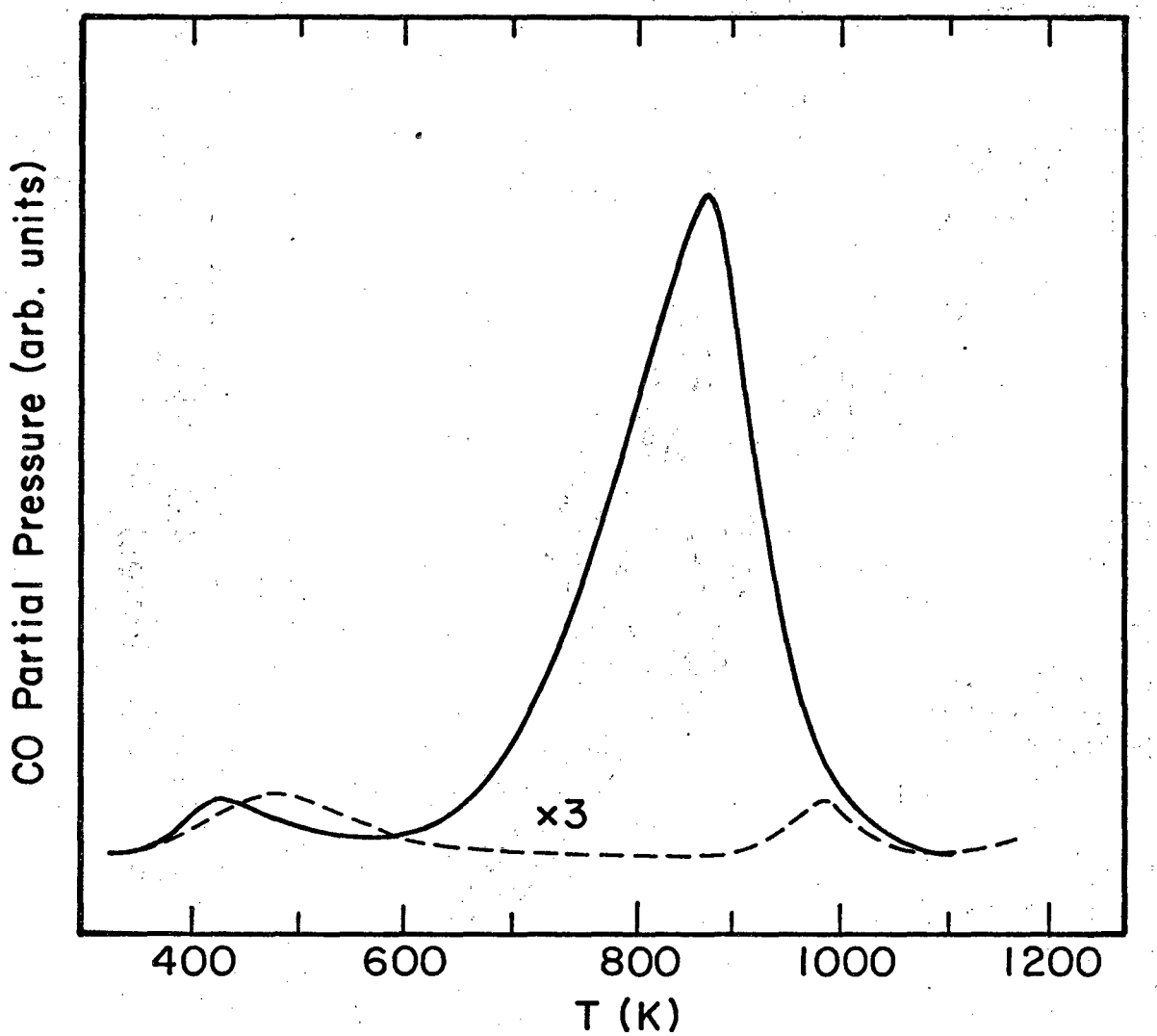

XBL 818-11315

Fig.5

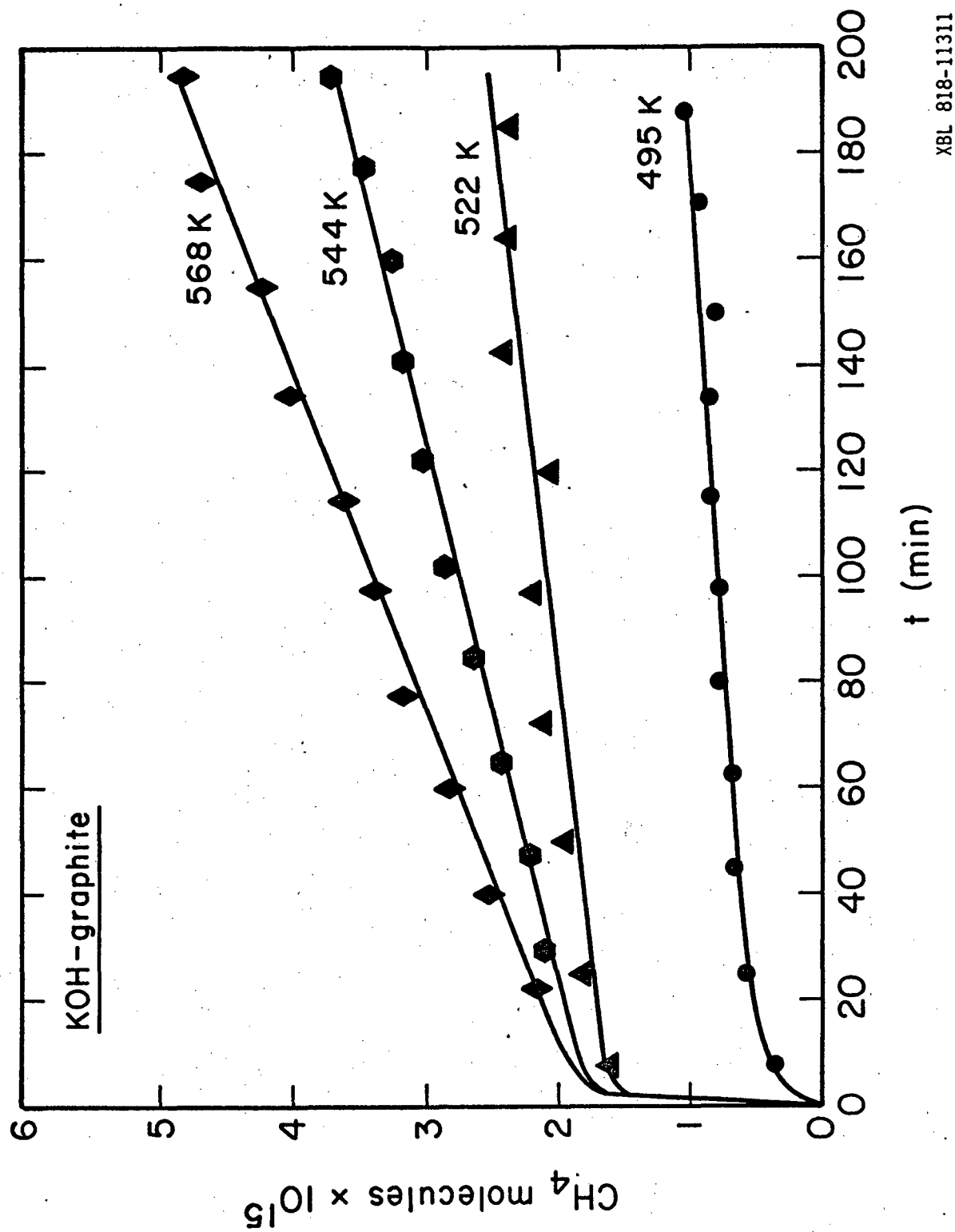

XBL 818-11311

Fig.6

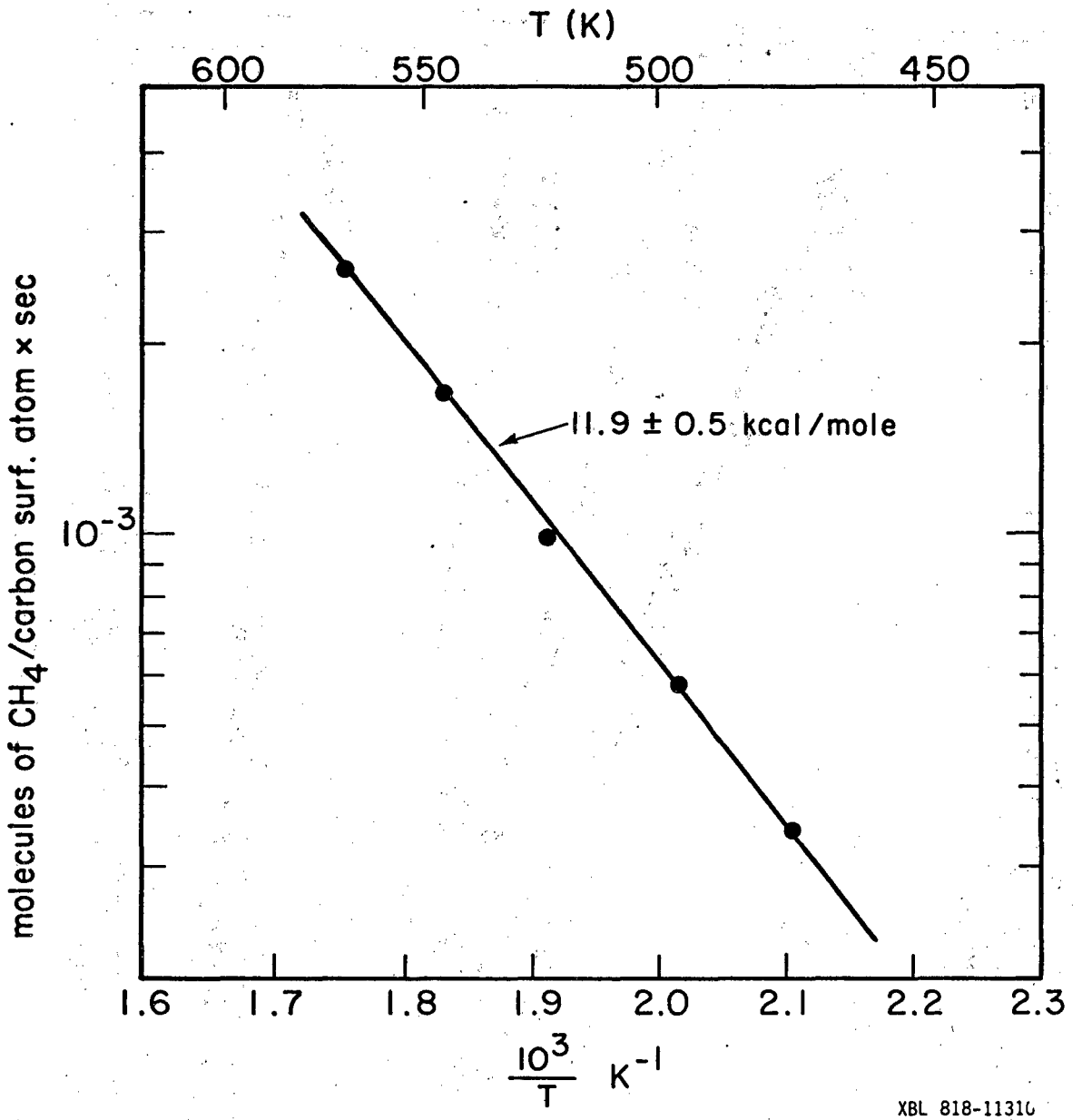
T (K)
600
550
500
450
11.9 ± 0.5 kcal/mole
10^{-3}
molecules of CH_4/carbon surf. atom × sec
1.6
1.7
1.8
1.9
2.0
2.1
2.2
2.3
$\frac{10^3}{T}$ K^{-1}
XBL 818-11310

Fig.7

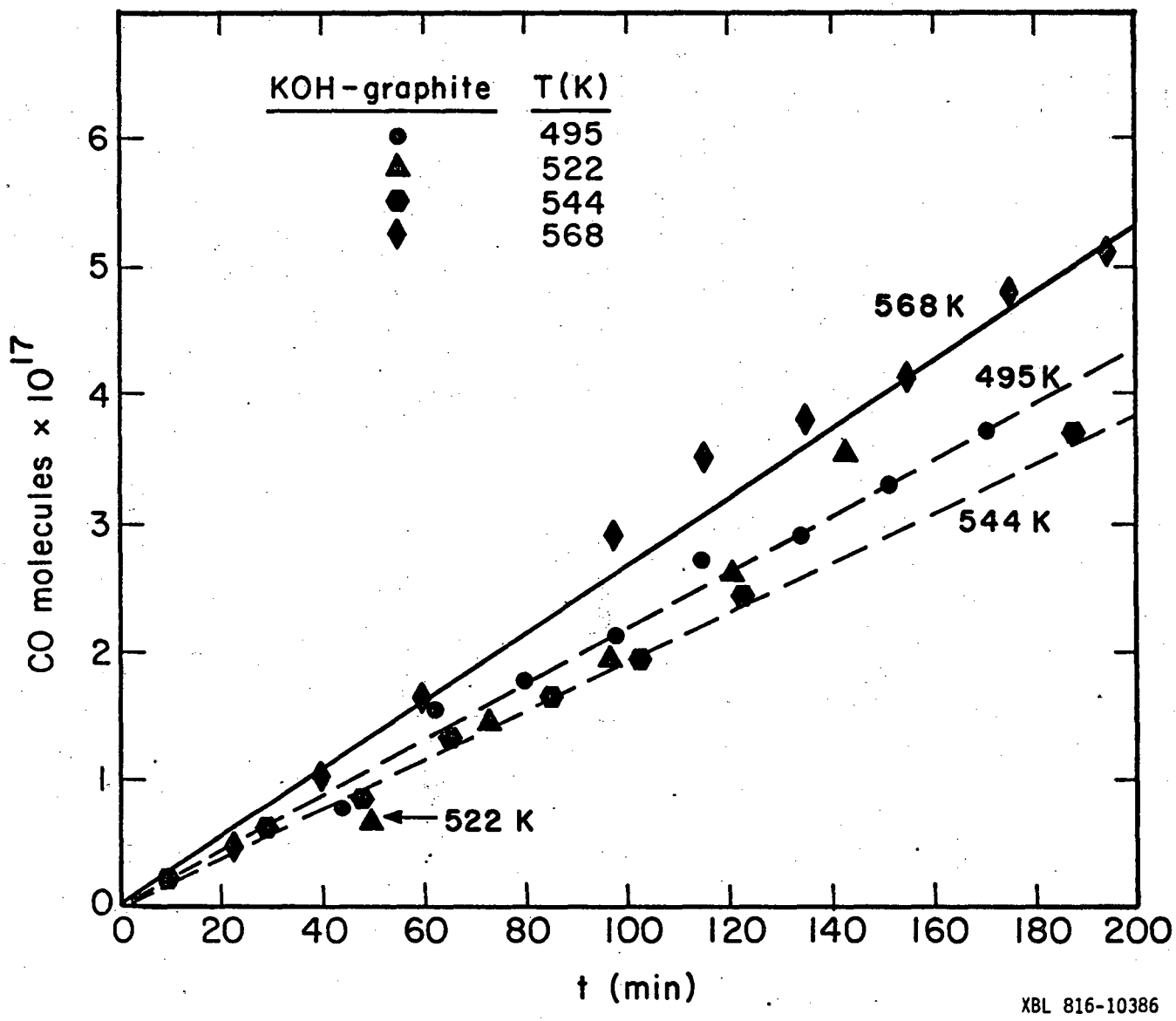
KOH-graphite
T(K)
495
522
544
568
568 K
495 K
544 K
522 K
CO molecules × 10^{17}
t (min)
0
1
2
3
4
5
6
0
20
40
60
80
100
120
140
160
180
200
XBL 816-10386

Fig. 8

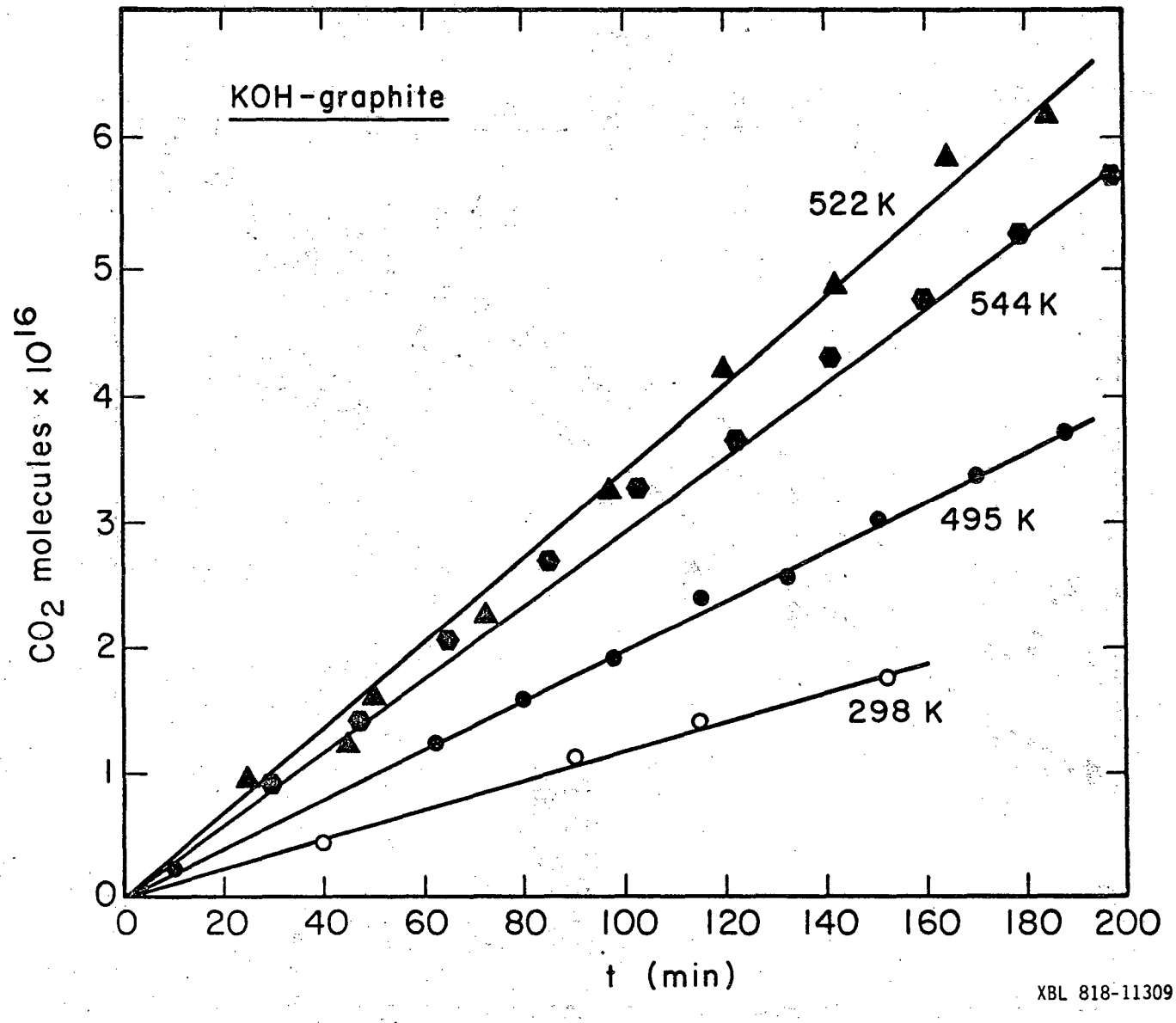
KOH-graphite
522 K
544 K
495 K
298 K
CO_2 molecules × 10^{16}
0
1
2
3
4
5
6
0
20
40
60
80
100
120
140
160
180
200
t (min)
XBL 818-11309

Fig.9

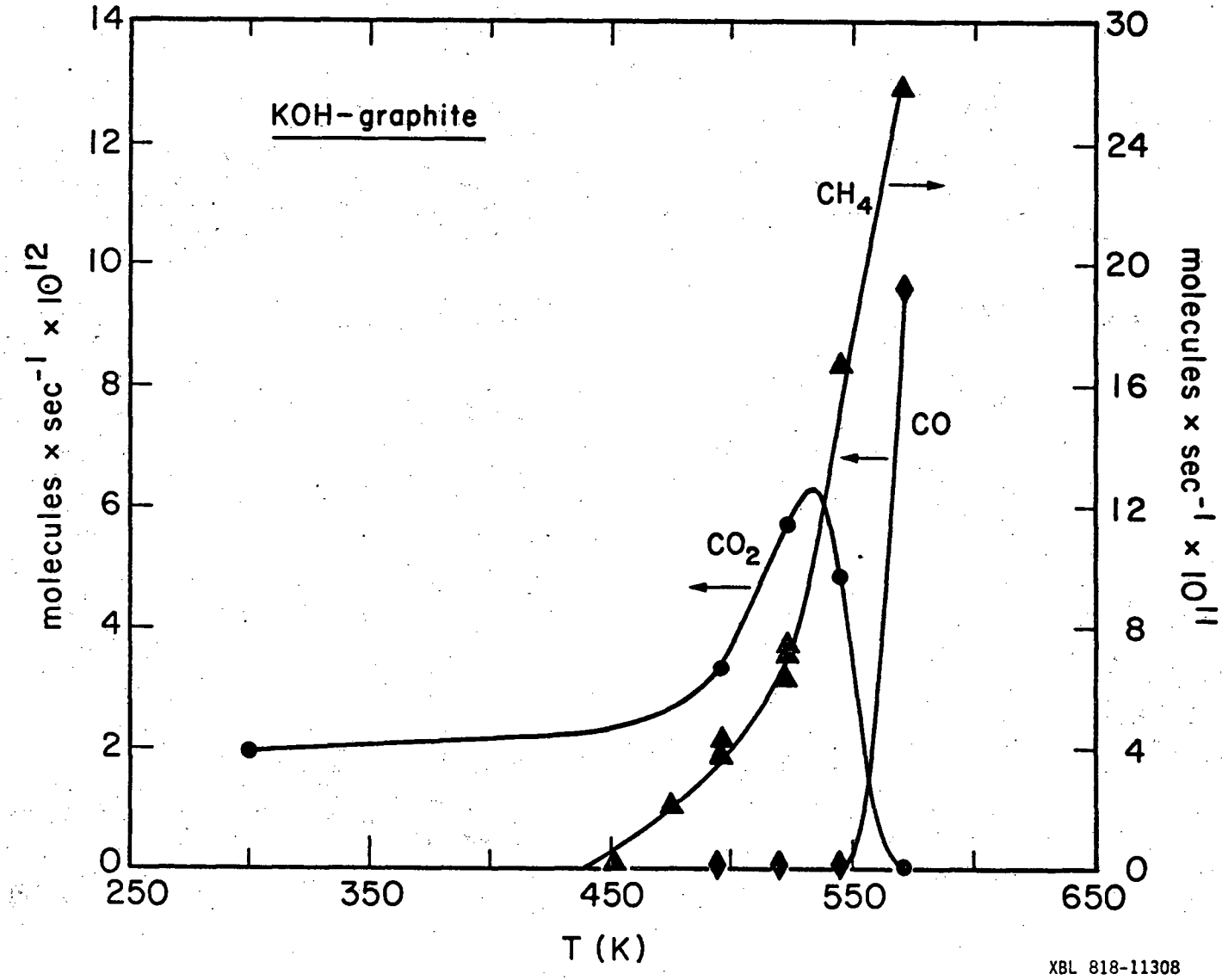
KOH-graphite
CH4
CO
CO2
molecules × sec-1 × 10^12
molecules × sec-1 × 10^11
T (K)
0
2
4
6
8
10
12
14
0
4
8
12
16
20
24
30
250
350
450
550
650
XBL 818-11308

Fig. 10

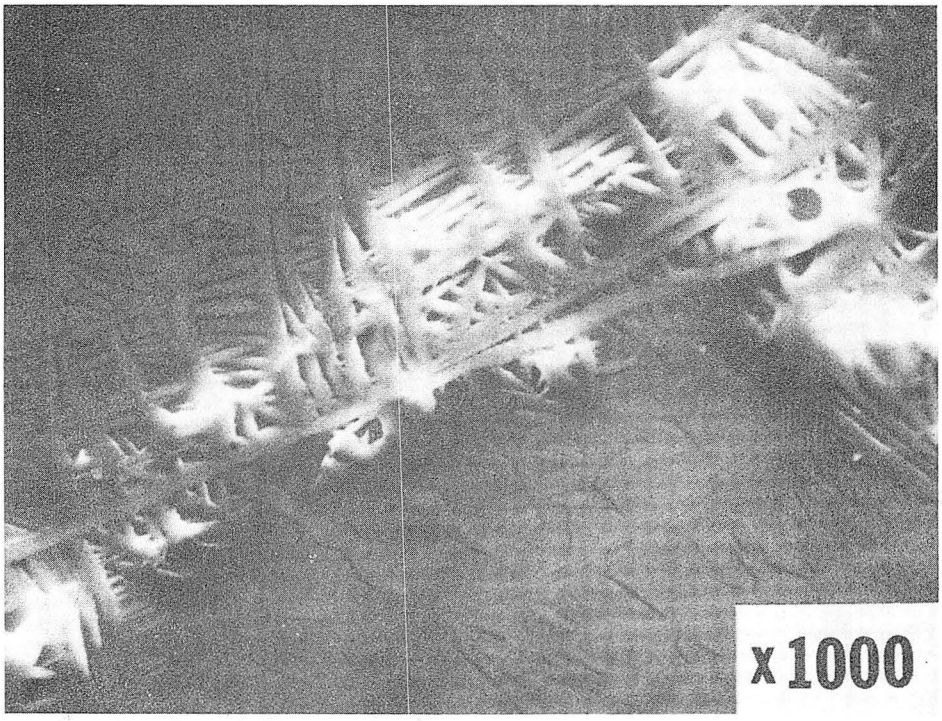

(a)

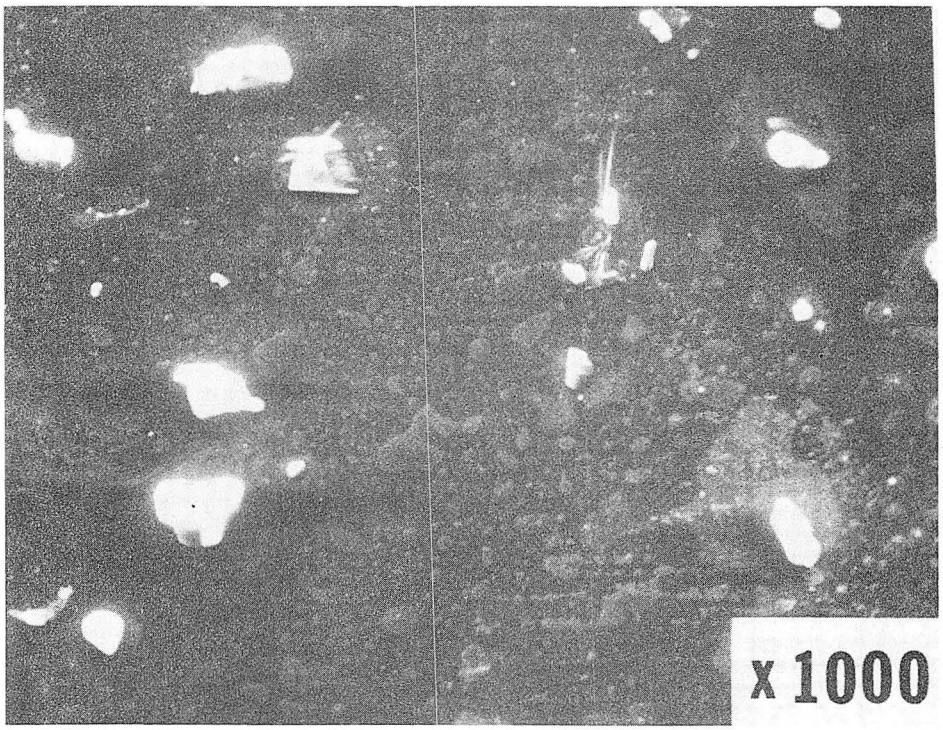

XBB 816-5635

(b)

Fig. 11

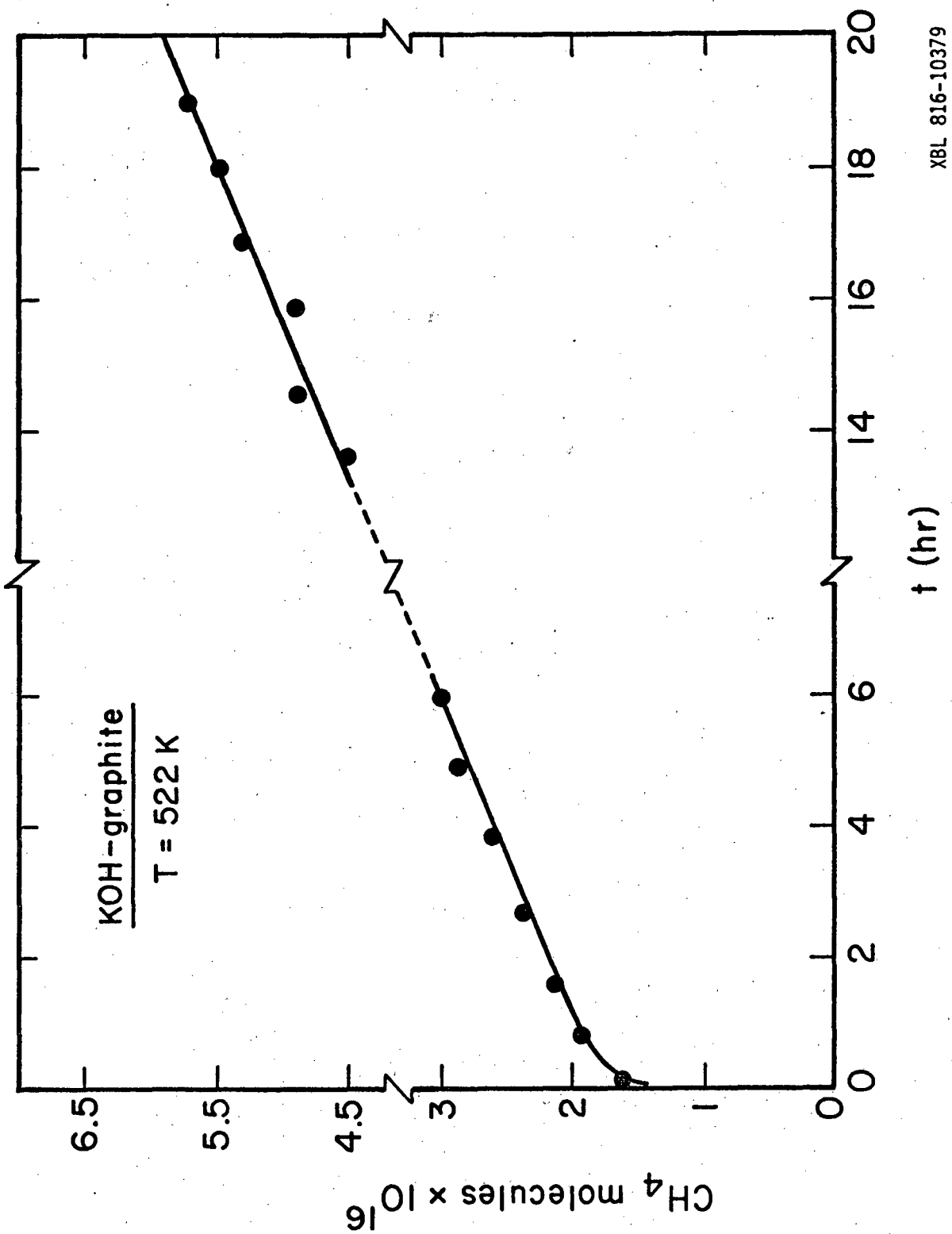
KOH-graphite
T = 522 K
CH4 molecules x 10^16
6.5
5.5
4.5
3
2
1
0
0
2
4
6
14
16
18
20
t (hr)
XBL 816-10379

Fig. 12

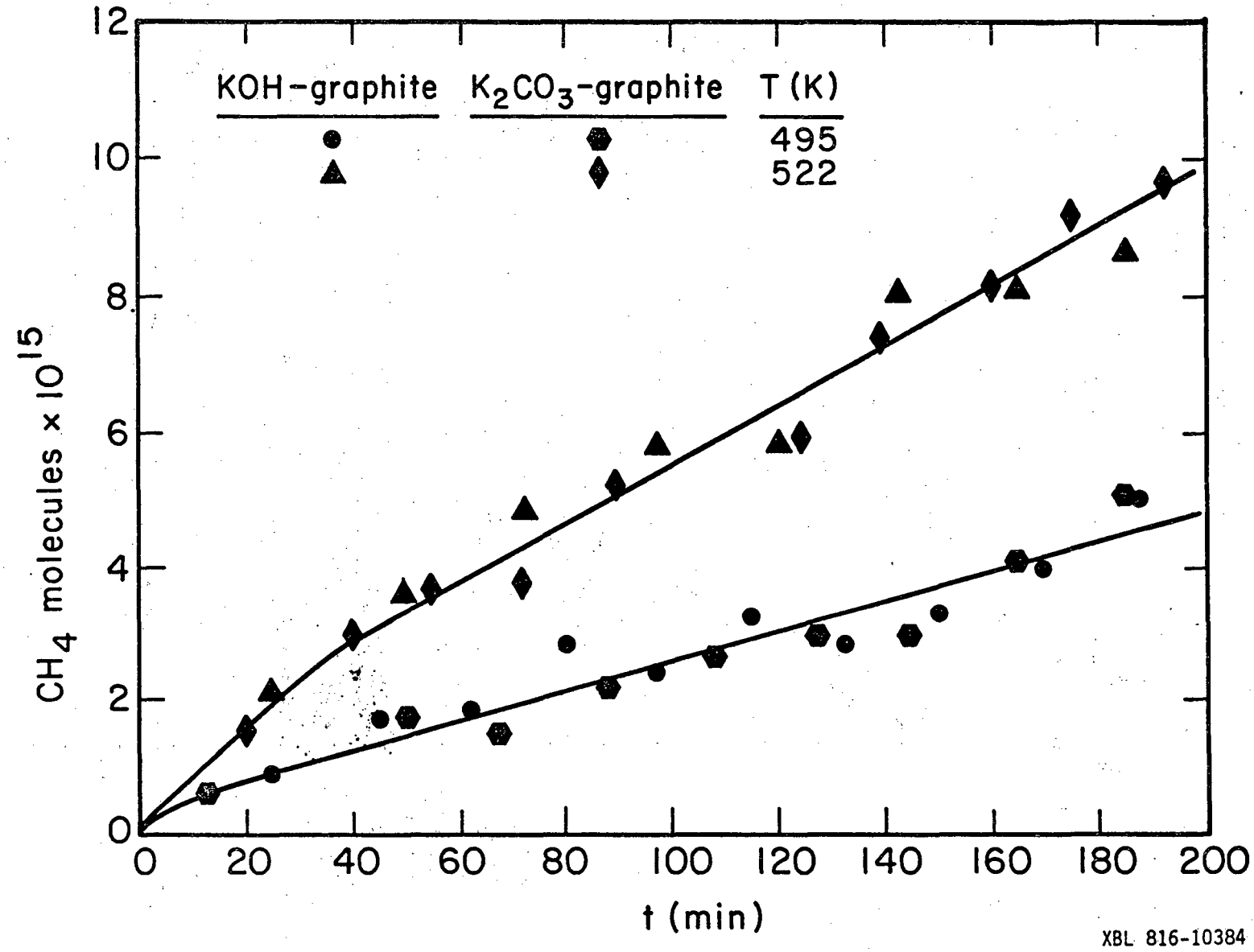
KOH-graphite
K_2CO_3-graphite
T (K)
495
522
CH_4 molecules × 10^{15}
t (min)
0
2
4
6
8
10
12
0
20
40
60
80
100
120
140
160
180
200
XBL 816-10384

Fig. 13

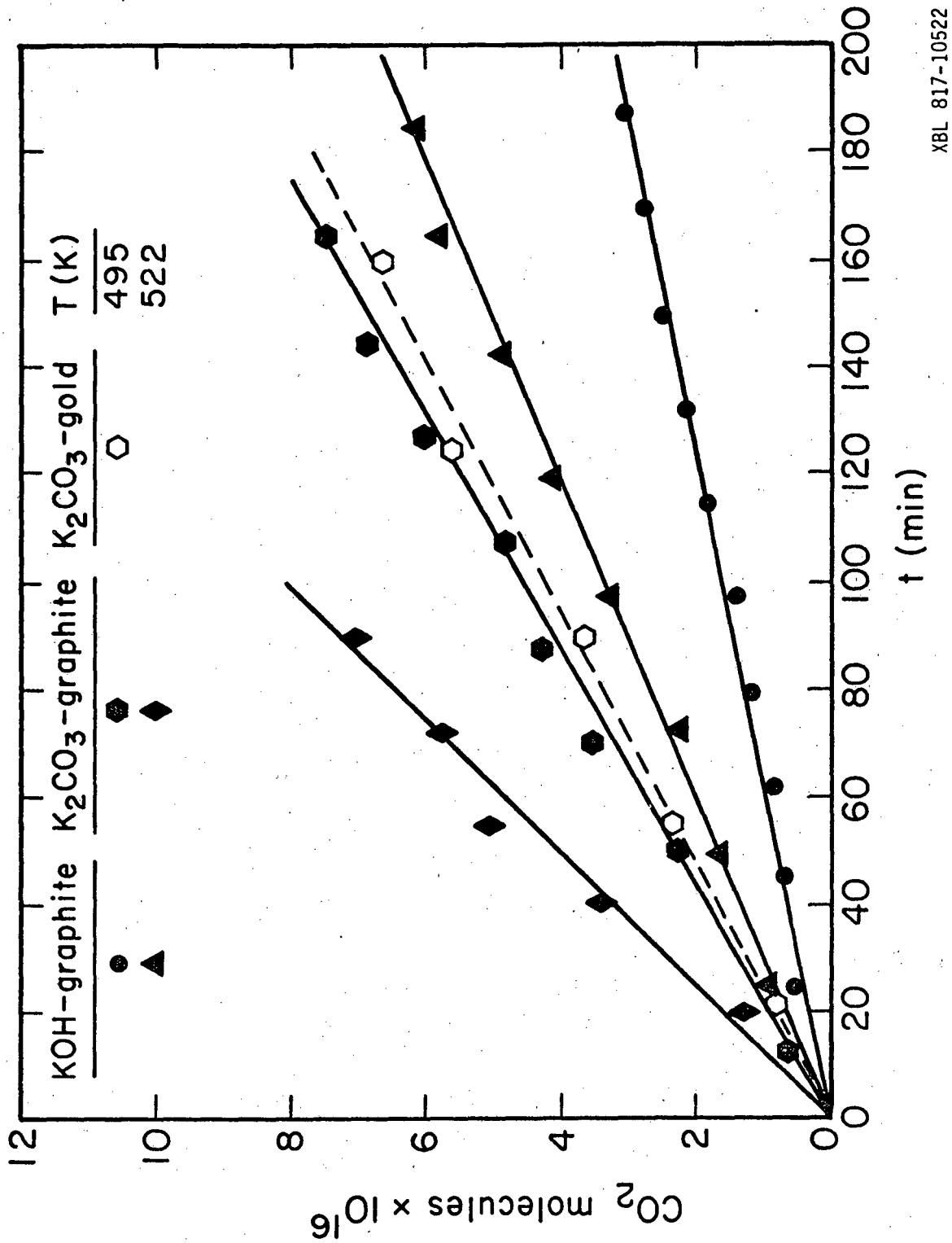
KOH-graphite
K_2CO_3-graphite
K_2CO_3-gold
T (K)
495
522
CO_2 molecules × 10^{16}
t (min)
0
2
4
6
8
10
12
0
20
40
60
80
100
120
140
160
180
200
XBL 817-10522

Fig. 14

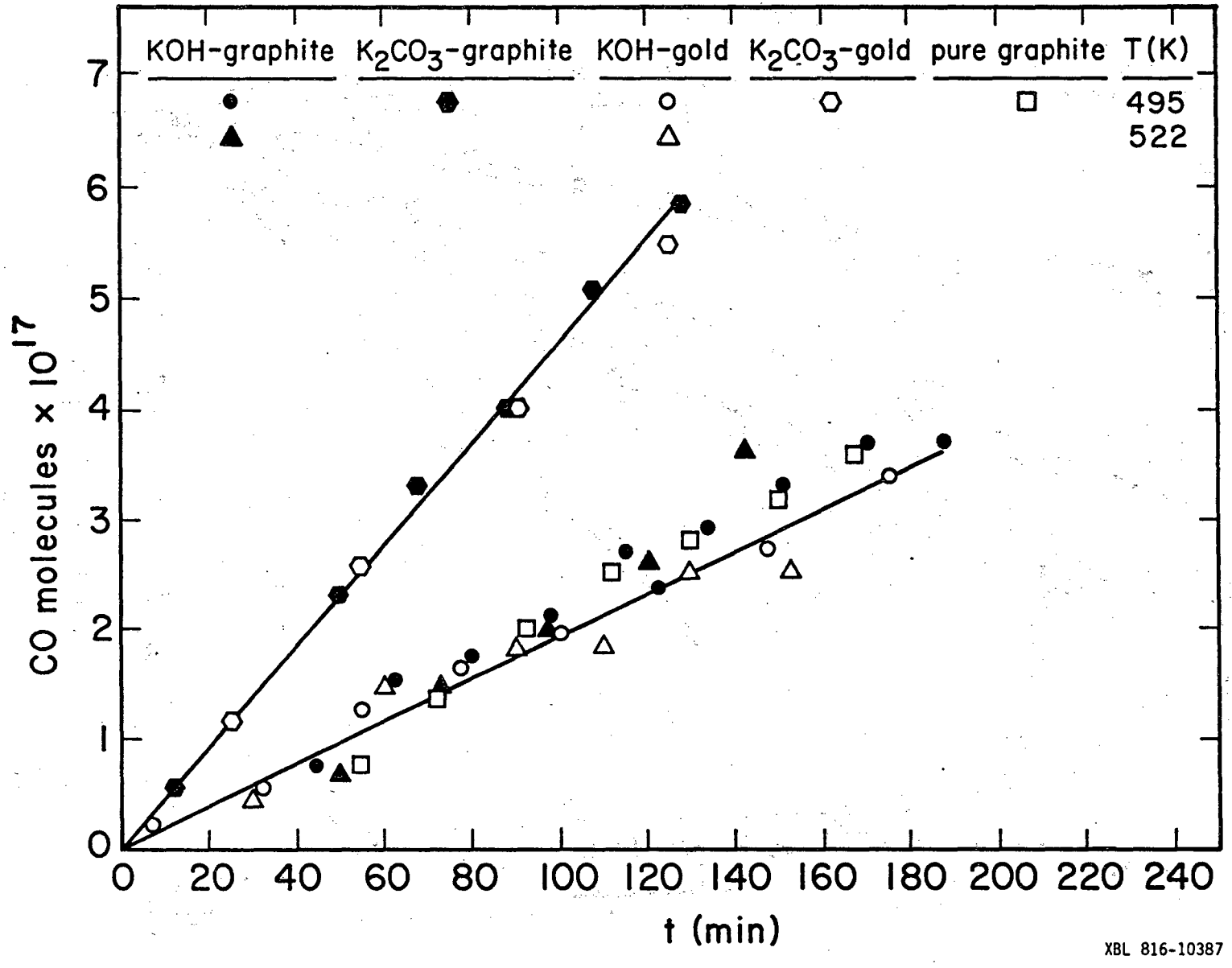

XBL 816-10387

Fig. 15

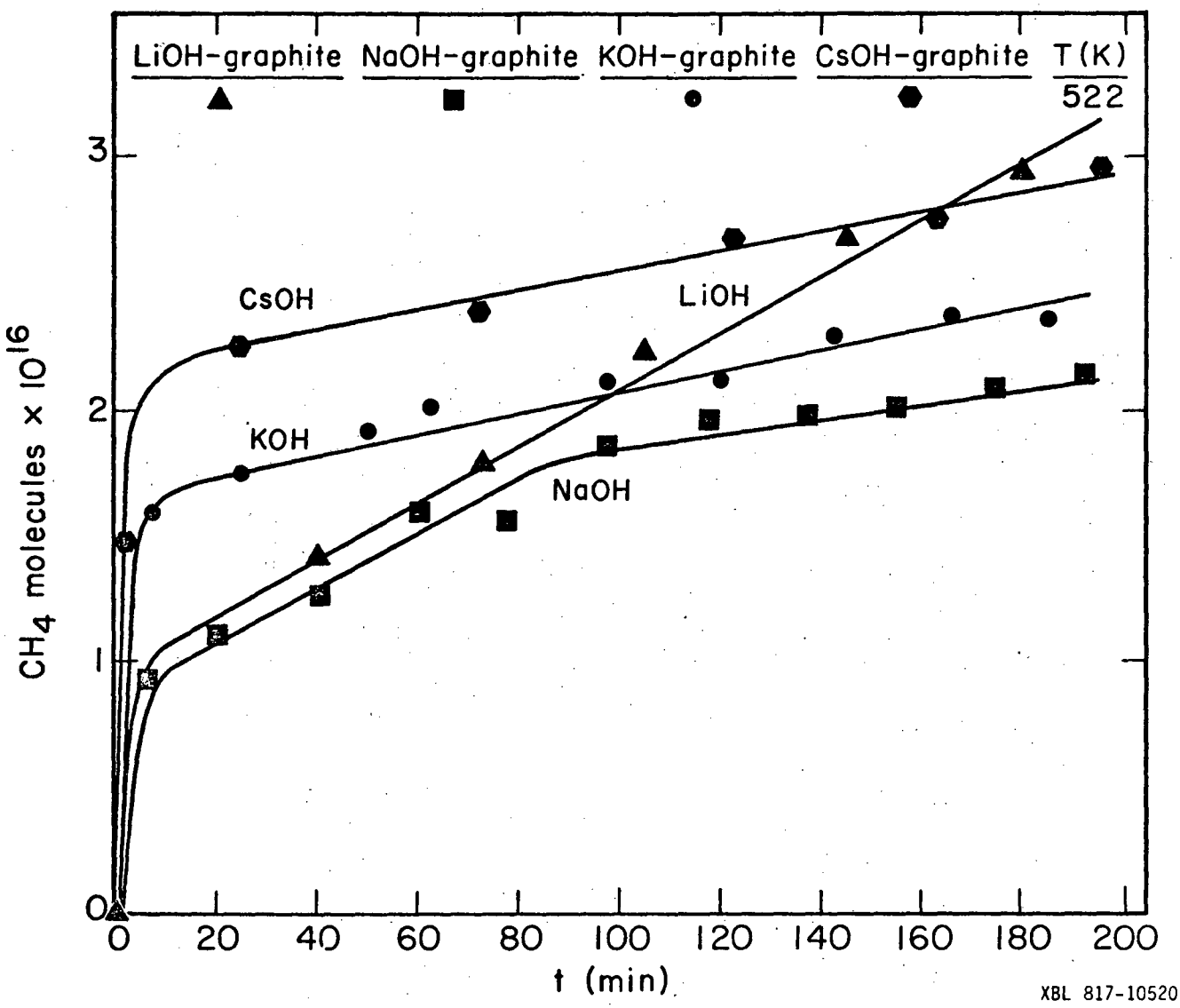
LiOH-graphite
NaOH-graphite
KOH-graphite
CsOH-graphite
T (K)
522
CsOH
LiOH
KOH
NaOH
CH_4 molecules x 10^{16}
t (min)
0
1
2
3
0
20
40
60
80
100
120
140
160
180
200
XBL 817-10520

Fig. 16

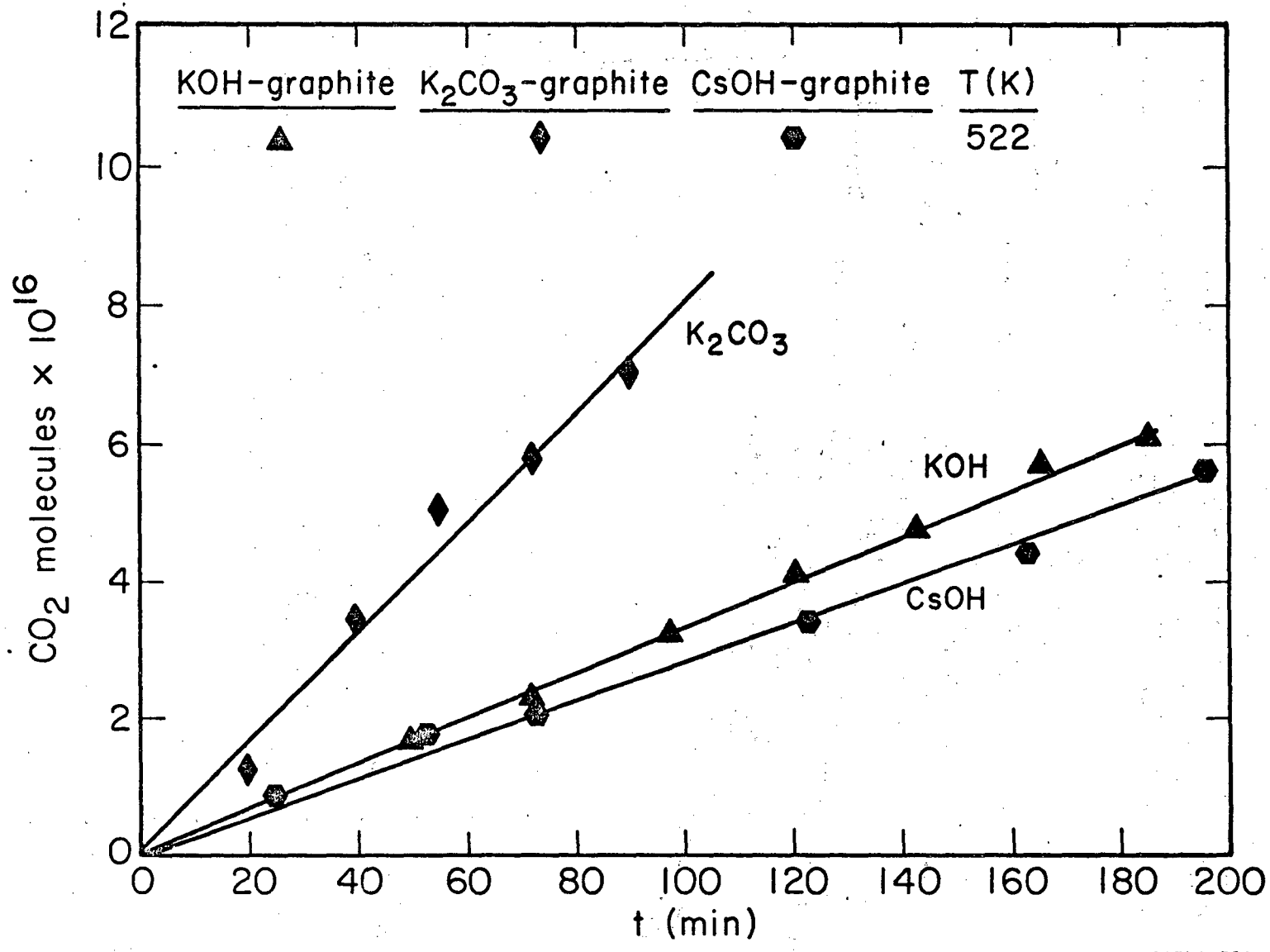

XBL 817-10521

Fig. 17

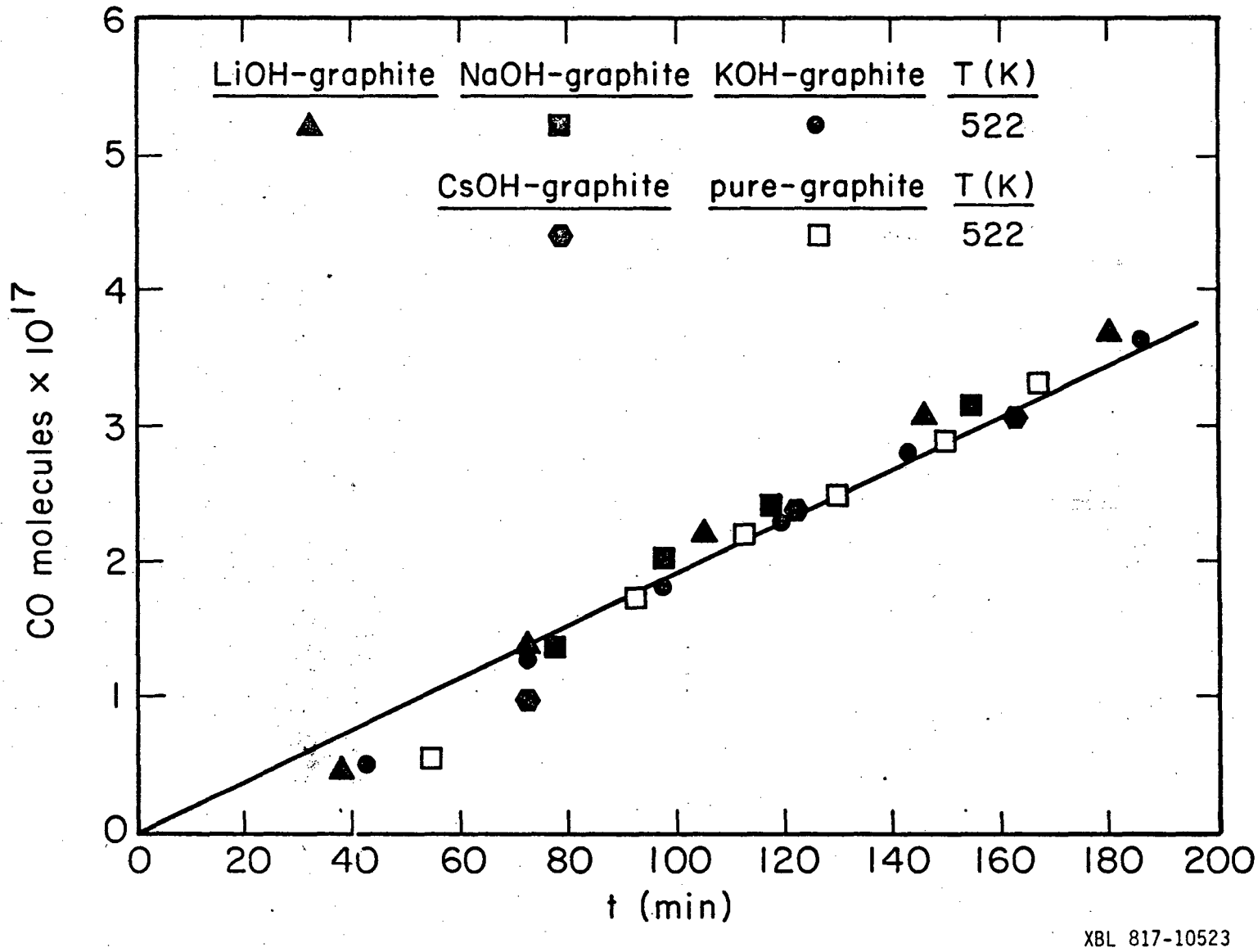
LiOH-graphite
NaOH-graphite
KOH-graphite
T (K)
522
CsOH-graphite
pure-graphite
T (K)
522
CO molecules × 10^17
t (min)
0
1
2
3
4
5
6
0
20
40
60
80
100
120
140
160
180
200
XBL 817-10523

Fig. 18

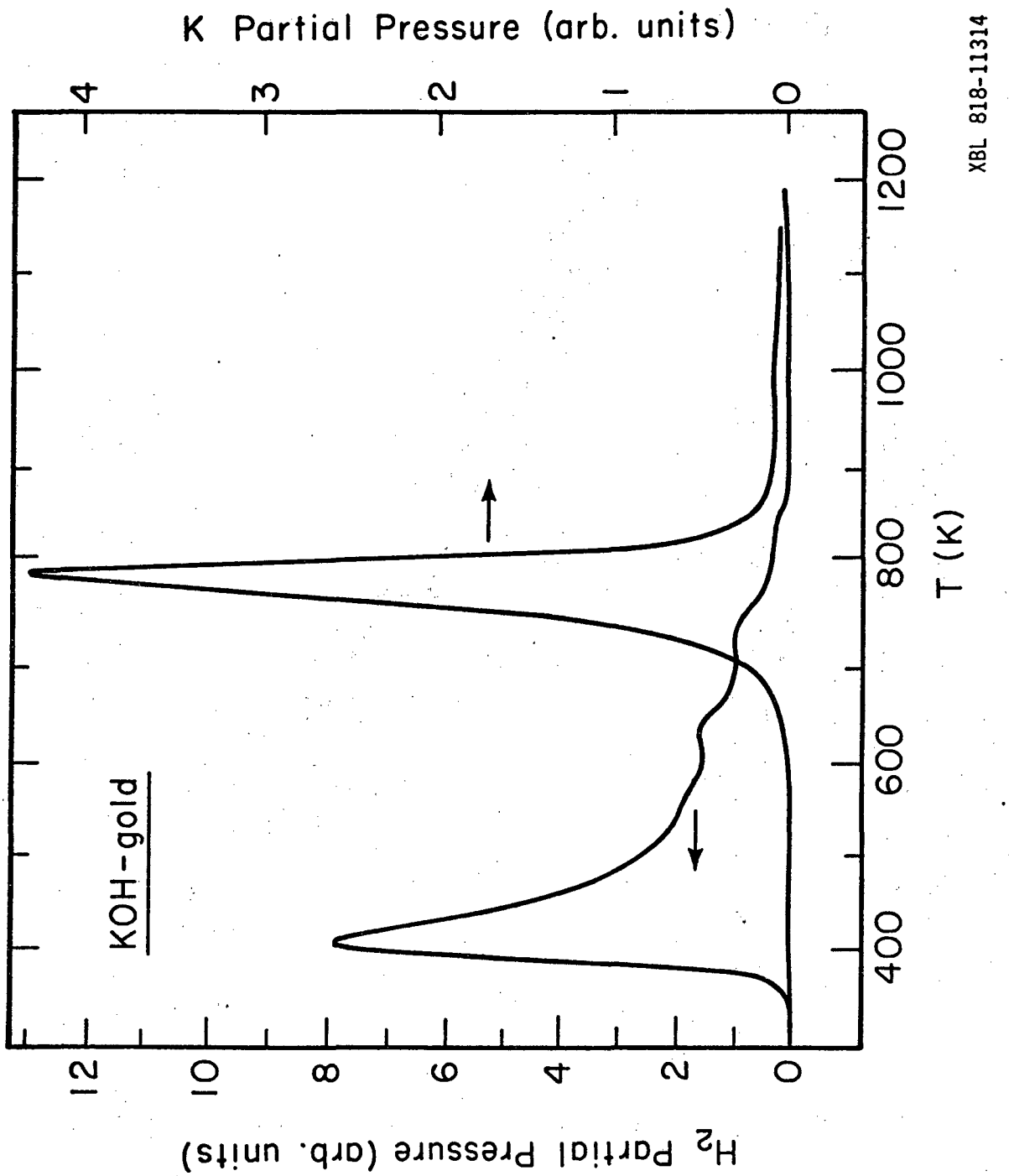

XBL 818-11314

Fig. 19

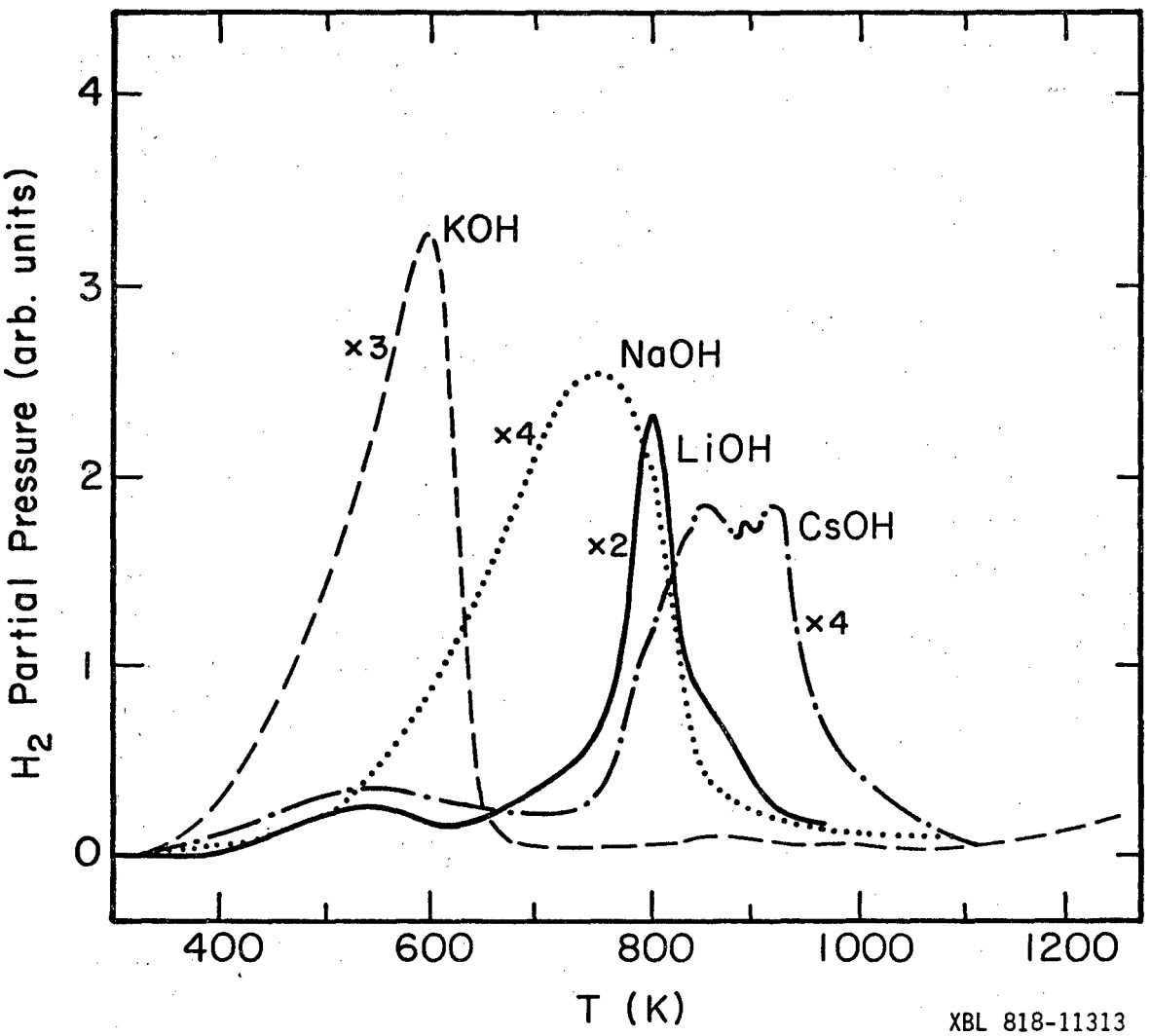
4
3
2
1
0
H_2 Partial Pressure (arb. units)
KOH
×3
NaOH
×4
LiOH
×2
CsOH
×4
400
600
800
1000
1200
T (K)
XBL 818-11313

Fig.20

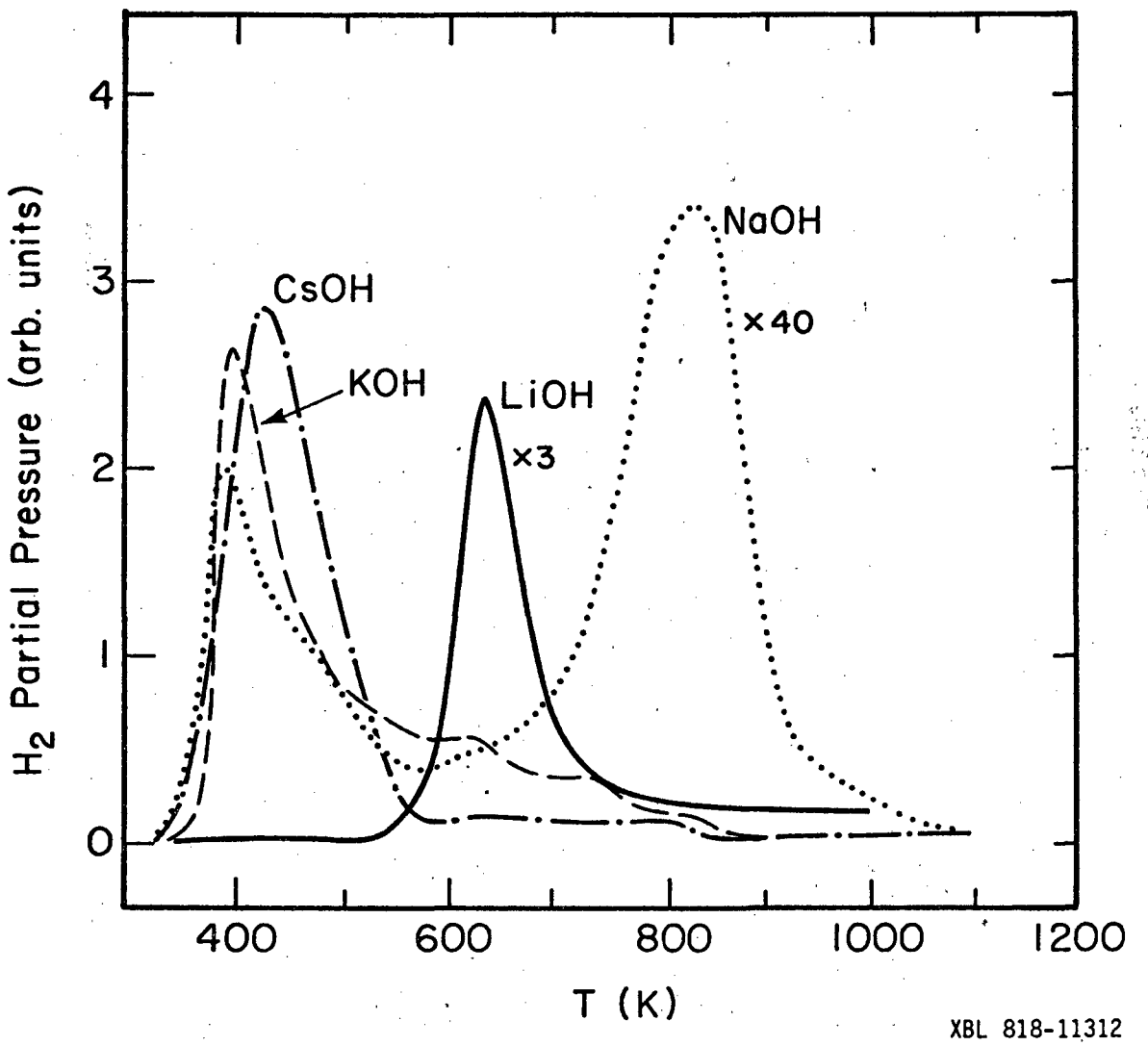
4
3
2
1
0
H_2 Partial Pressure (arb. units)
CsOH
KOH
LiOH
×3
NaOH
×40
400
600
800
1000
1200
T (K)
XBL 818-11312

Fig.21

This report was done with support from the Department of Energy. Any conclusions or opinions expressed in this report represent solely those of the author(s) and not necessarily those of The Regents of the University of California, the Lawrence Berkeley Laboratory or the Department of Energy.

Reference to a company or product name does not imply approval or recommendation of the product by the University of California or the U.S. Department of Energy to the exclusion of others that may be suitable.

TECHNICAL INFORMATION DEPARTMENT
LAWRENCE BERKELEY LABORATORY
UNIVERSITY OF CALIFORNIA
BERKELEY, CALIFORNIA 94720